

## Chapter 5

### **Electrochemistry, Spectroelectrochemistry and Monolayer Formation of a Tetrathiafulvalene derivative: 5,6 – dehydro-5,6-di(pyrid-4-yl)- bis(ethylenedithio)tetrathiafulvalene**

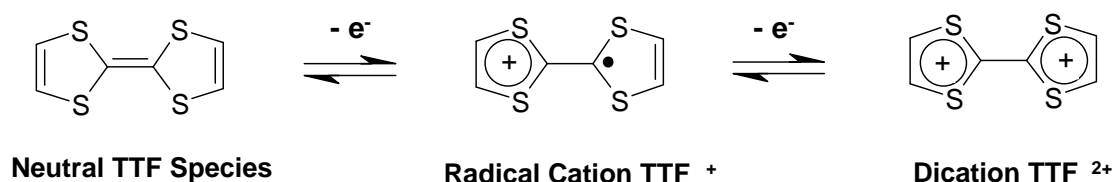
*The electrochemical properties of an organic redox active molecule, dipyrBEDT-TTF have been examined using cyclic voltammetry and differential pulse voltammetry. Two reversible anodic processes and two irreversible cathodic processes are observed for this compound. The neutral molecule is initially oxidised to a monocation radical with a second oxidation resulting in a dication. The stability of the monocation redox intermediate is dependent on the Gutmann donor number of the electrochemical solvent; the stability of the monocation redox intermediate decreases as the Gutmann donor number increases. The dication is stable in an anaerobic environment; however, the presence of oxygen causes a proceeding chemical reaction leading to the degradation of the dipyrBEDT-TTF compound. The monocation is stable in both the presence, and absence, of oxygen as verified via spectroelectrochemistry. Several different conditions for the formation of a monolayer of the species on Pt and Au have been explored. A monolayer formed at a Pt electrode exhibited increased stability when the electrochemical measurements were carried out in the absence of oxygen. The values obtained for  $\Delta E$  and the FWHM suggest that repulsive lateral interactions may be present within the monolayer.*

## 5.1 Introduction

### 5.1.1 Molecular Rectifiers

As current advances in the information technology semiconductor industry draw closer and closer to the ever more prominent limits, replacement of the ‘silicon chip’ becomes more and more pressing. Following the ‘*bottom-up*’ approach, first proposed by Richard P. Feynman<sup>1</sup> in 1960, the potential for possible alternatives to the current electronic devices arose and with them the anticipation of a new era in the world of information storage and processing.

The realization of molecular diodes (rectifiers) is central to the development of molecular electronic devices. Shortly after Wudl *et al.* first reported the synthesis and characterisation of the core tetrathiafulvalene compound (TTF)<sup>2</sup> the possibility for molecular rectification through this type of system was proposed. Aviram and Ratner<sup>3</sup> postulated that molecular rectifying behaviour could be achieved through a single organic molecule based on a donor (D)-spacer-acceptor (A) model (*vide infra*). The organic sulphur heterocyclic TTF (2,2'-bis(1,3-dithiolylidene)), is an electron rich alkene and is oxidised in two steps; the first oxidation produces a radical cation followed by the formation of a dication as the second step, Scheme 5.1.<sup>4,5</sup>



**Scheme 5.1:** Electrochemical oxidation of the neutral TTF molecule to the mono- and dication species.<sup>6</sup>

Single crystals of TTF were studied using X-ray crystallography.<sup>7</sup> The formation of the molecules, where the central double bonds are lined up along the crystal’s axes, provoked the idea that conduction may be possible within this molecule if placed in an electric field: semiconductor behaviour was observed at room temperature providing the molecule was kept in the dark.<sup>2b</sup>

There are several advantages of using the TTF core as a building block for more advanced materials: upon oxidation of the TTF ring system, a thermodynamically stable cation radical is formed and further oxidation results in the dication; both of these processes are reversible and occur within an accessible potential window forming stable redox states. By adding electron donating/withdrawing groups to the TTF core, the oxidation potentials can be tuned.<sup>8</sup> TTF derivatives are famous for their  $\pi$ -electron donor capabilities. This is partly due to the aromatization energy gain when going from the neutral species to the dithiolium aromatic rings in the singly and doubly oxidised states, Scheme 5.1.

In 1973 Cowen *et al.*<sup>9</sup> discovered metallic conductivity in the novel donor – acceptor complex consisting of TTF as the donor and tetracyano-*p*-quinodimethane as the acceptor, Figure 5.1. At the time this complex not only exhibited metallic properties over a large temperature range but also possessed the largest electrical conductivity of any known organic compound.

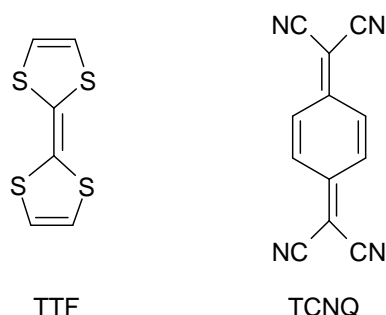


**Figure 5.1:** Molecular structures of TTF and TCNQ.

Following on from the disclosure of this TTF/TCNQ system, Aviram and Ratner went one step further and discussed the possibility of a similar system for potential applications in molecular electronics; in particular molecular rectifiers.<sup>3</sup> Their idea was based around the donor  $\pi$ - and acceptor  $\pi$ -systems, Figure 5.1, with both units connected via a  $\sigma$ -bonded non-conjugated bridge (TTF- $\sigma$ -TCNQ, Figure 5.2): the donor and acceptor properties of the subunits can be increased or decreased depending on the electron donating/withdrawing properties of additional substituents on the aromatic units. The purpose of the spacer between the donor and acceptor moieties is to provide sufficient charge separation which is achieved through the use of  $\sigma$ -bonds

whereas the delocalized orbitals on the  $\pi$  bonds allow for conductivity through the spacer and hence the flow of a current.<sup>10</sup> When spaced between two electrodes, electron flow will occur in one direction only. Solid state rectifiers employ p-n junctions: it was proposed that an organic system operating on the same principle, containing electron poor (p-type) and electron rich (n-type) components, would exhibit properties of a molecular rectifier.

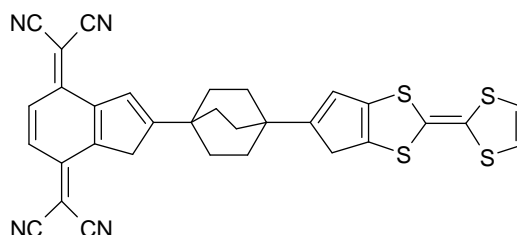


**Figure 5.2:** Aviram and Ratner model of a molecular rectifier, TTF- $\sigma$ -TCNQ.<sup>3</sup>

When placed between two metal electrodes, and applying a potential, the asymmetry of the donor and acceptor orbitals determines that the flow of current is unidirectional. Electrons can flow from the cathode to the acceptor and consequently electrons are transferred from the donor to the anode.<sup>11</sup> Rectifier behaviour is brought about when, at an appropriate voltage, electrons and holes are released into the molecule's LUMO and HOMO levels, located on the TCNQ and TTF units respectively,<sup>10</sup> from the Fermi levels of the enclosing electrodes resulting in the charge separated species TTF<sup>+</sup>- $\sigma$ -TCNQ<sup>-</sup>. It is this charge separated species that would allow electron tunnelling through the  $\sigma$ -spacer and hence current (electrons) flowing in the acceptor – donor direction.<sup>12</sup>

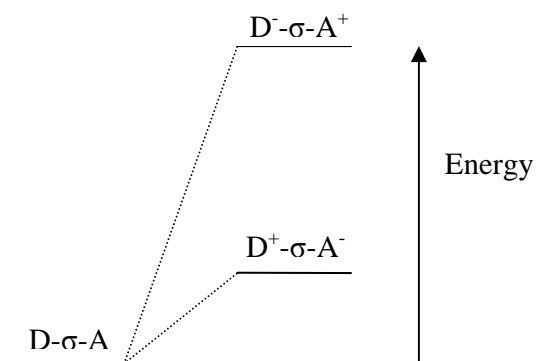


**Figure 5.3:** Energy difference between the D<sup>+</sup>- $\sigma$ -A<sup>-</sup> and D<sup>-</sup>- $\sigma$ -A<sup>+</sup> states.

The energy required for the formation of this  $D^+-\sigma-A^-$  zwitterion is 3.5 eV. In this model for current to flow in the reverse direction the application of a much higher potential (9.6 eV) is required in order to move an electron and create the  $D^--\sigma-A^+$  zwitterionic state.<sup>13</sup> This is because of the larger gap between the low energy local HOMO orbital of the acceptor and the high energy local LUMO orbital of the donor functionality.

Although the proposed TTF- $\sigma$ -TCNQ compound has not yet been synthesised, several similar compounds based on this type of D- $\sigma$ -A model have been reported.<sup>12, 13, 14</sup> One example was reported in 2005 by Heath *et al.*<sup>12</sup> showing unimolecular rectifier behaviour that incorporated a TTF group as the donor and a fluorene as the acceptor with a saturated bridge in between (see Chapter 1). This compound exhibits a low HOMO-LUMO energy gap of approximately 0.3 eV and Langmuir-Blodgett monolayers of this complex were formed which increased the rectifier behaviour.

The Aviram and Ratner D- $\sigma$ -A model presents a solution for the realization of a molecular rectifier. However, problems still arise with these types of complexes: synthetic challenges remain even today with the covalent linking of the TTF and TCNQ compounds; only a few single crystal x-ray structures of these types of systems are reported and evidence for intervalence charge transfer is lacking.

### 5.1.2 Bis(ethylenedithio)tetrathiafulvalene (BEDT-TTF) Compounds

A wide variety of bis(ethylenedithio)tetrathiafulvalene (BEDT-TTF) compounds have been synthesised and reported in the literature.<sup>15</sup> These compounds are of particular interest because of their broad range of electrical properties and their application in molecular conductors and superconductors.<sup>16, 17</sup> The properties of the BEDT-TTF compound have been tuned by creating derivatives using several types of organic substituents including alkyl chains, aryl, halo and carbonyl groups, and in the case of the compound discussed in this chapter pyridyl functionalised BEDT-TTF compounds have also been reported.<sup>15a, c, f, g</sup> An attractive feature of these types of compounds is their ability to transform into metals and in some cases superconductors when converted to their radical cation salts.

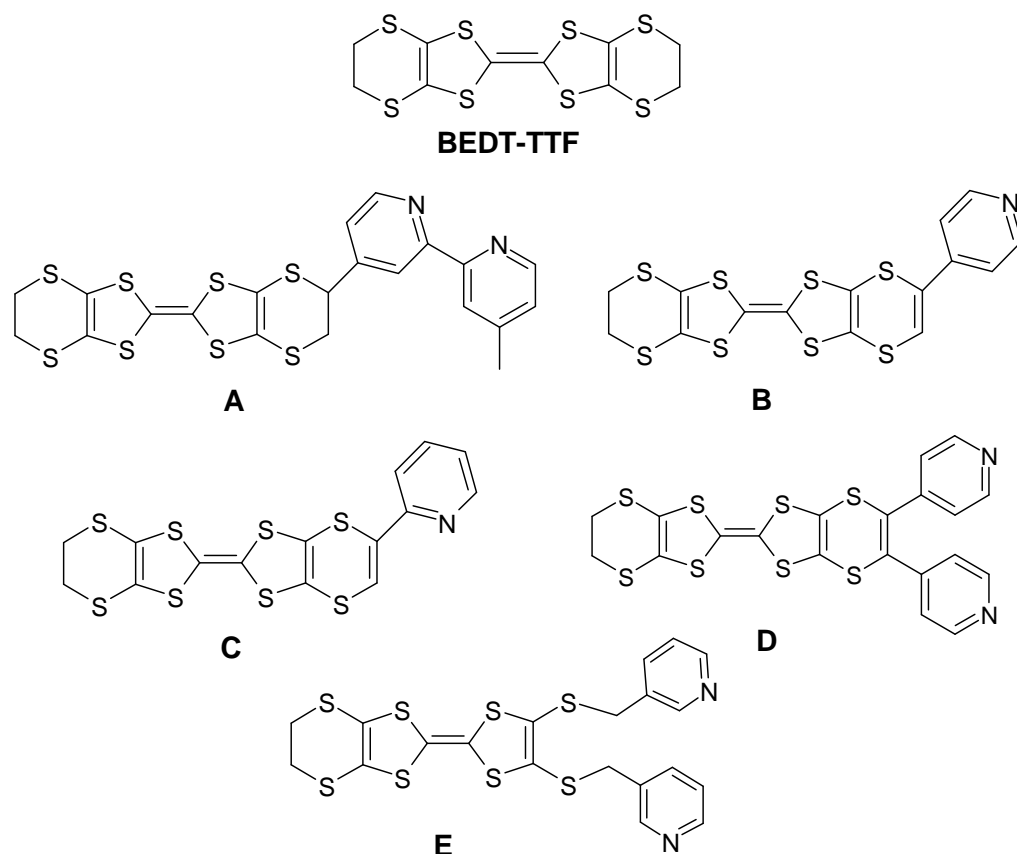


**Figure 5.4:** Molecular structure of BEDT-TTF and related pyridyl functionalised TTF derivatives. .

Compound	$E_{1/2}$ [V]	Reference
A	+0.55, +0.95	Ouahab <i>et al.</i> <sup>18</sup>
B	+0.50, +0.89	Xu <i>et al.</i> <sup>15g</sup>
C	+0.48, +0.89	Xu <i>et al.</i> <sup>15g</sup>
D (dipyrBEDT-TTF)	+0.73, +1.05	Wallis and Almeida <i>et al.</i> <sup>15a</sup>
E	+0.54, +0.90	Zhu <i>et al.</i> <sup>19</sup>
BEDT-TTF	+0.52, +0.94	Ouahab <i>et al.</i> <sup>18</sup>
TTF	+0.32, +0.76	Wudl <i>et al.</i> <sup>6,</sup>

**Table 5.1:** Half-wave potentials of TTF, BEDT-TTF and pyridine substituted derivatives. The oxidation potentials have been corrected against the SCE reference electrode. The electrochemistry of these compounds was recorded in  $CH_2Cl_2$  apart from TTF which was recorded in ACN.

The redox potentials of TTF and BEDT-TTF, as well as derivatives of the latter with one or more pyridine rings attached, are presented in Table 5.1. The addition of the ethylenedithio groups to the TTF central core unit results in an increase in the oxidation potentials with positive shifts in the region of 200 mV observed for BEDT-TTF compared to TTF alone; electron density is pulled away from the redox sites of the TTF core as a result of the electron withdrawing properties of the outer ethylenedithio groups.

The effect of addition of a pyridine ring to the BEDT-TTF compound appears to give conflicting results depending on the compound in question. Ouahab *et al.* report that the bipyridine substituent has a negligible effect on the redox chemistry and that the observed difference in potentials between **A** and BEDT-TTF lie in the region of experimental error.<sup>18</sup> In contrast to this, Xu *et al.*,<sup>15g</sup> and Wallis and Almeida *et al.*<sup>15a</sup> report an increase in redox potential upon addition of pyridine rings to the BEDT-TTF compound with the positive shift being greater in the case of the latter. This can be explained by the electron withdrawing properties of the pyridine rings; in compound **D** (dipyrBEDT-TTF) there are two pyridine rings bonded to the central unit and as a result there is less electron density located at the redox sites of the core TTF unit and therefore a greater increase in oxidation potential is observed. The nitrogen atom of the pyridine ring of **B** is in the para- position whereas in compound **C** it is located in the ortho- position. From the oxidation potentials of both **B** and **C** it is observed that the substituent position does not significantly affect the oxidation potentials of the compounds.

### 5.1.3 D- $\alpha$ -A vs. Redox Controlled Conductance in Molecular Electronics

The donor compound, TTF and its derivatives have featured extensively in the literature concerning the notion of achieving rectifier behaviour based on the D- $\sigma$ -A system.<sup>8</sup> The main concept in these types of systems is the passage or transport of charge (electrons) from the acceptor, to the donor unit across a non-conjugated bridge in the form of intramolecular charge transfer. When these molecules are positioned between two enclosing electrodes a conducting species results, the behaviour of which

resembles that of a molecular rectifier in which current will only flow in one direction as a result of the different HOMO and LUMO energy levels of the donor and acceptor units.<sup>3, 10, 12</sup>

Using electrochemical techniques, the charge transport across single molecules can be controlled through switching from one redox state to the next.<sup>20, 21</sup> Single molecules can behave in different manners akin to those of electronic devices such as on-off switching transistor properties and rectification. Such characteristics are linked with the redox levels in the molecule and their resonance with the Fermi levels of the enclosing electrodes. This is not observed in non-redox molecules where the HOMO and LUMO levels are off-resonance with the Fermi levels of the electrodes.<sup>20c</sup> It has been demonstrated recently that this single molecule conductance phenomenon has not only been achieved in a vacuum but also in aqueous electrolyte.<sup>20, 21e-g</sup>

Oxidation of TTF complexes and their derivatives results in the formation of a cation radical followed by a dication. Two stable redox states also feature in organic complexes containing a viologen moiety where a dication is reduced to the monocation and subsequently the neutral species.<sup>20, 21b, 22</sup> Electrochemical *in situ* scanning tunnelling microscopy (STM) techniques, using a four-electrode configuration, have been used to demonstrate how the electrochemical potential can control the redox state of a viologen group, with alkane thiol chains at each end. A molecular wire consisting of gold at either end (from the substrate and STM tip) is presented and the viologen moiety acts as a “gate” for the charge transport across the molecular bridge. The low lying redox states of the viologen core (-0.42 and -0.90 V vs. SCE) provide a means for the mediation of electron transport through the two step reduction of the dication to the neutral species with changes in the electronic structure of the molecule.<sup>20</sup>

This research carried out on the viologen compound and its derivatives has successfully shown that electrochemical techniques can be used to control the electrical behaviour of molecules which are potentially useful as molecular electronic devices. Experiments using STM, for example, can lead to characterisation of electrical properties of redox processes in molecules by examining the relationship between the redox states and the observed conductance within the molecule. A similar

compound, containing a TTF core (Figure 5.5) has been reported by Ulstrup *et al.*<sup>23</sup> where electrochemical *in situ* STM measurements have shown that as the electrochemical gating potential sweeps through the different redox modes, a sharp “off-on-off” transition results. In contrast, the viologen analogue, 6V6<sup>20</sup> (Figure 5.5), exhibits a broader “off-on” switching profile. Since both compounds only vary in the central redox unit, the difference in conductivity is assumed to arise from this part of the system.

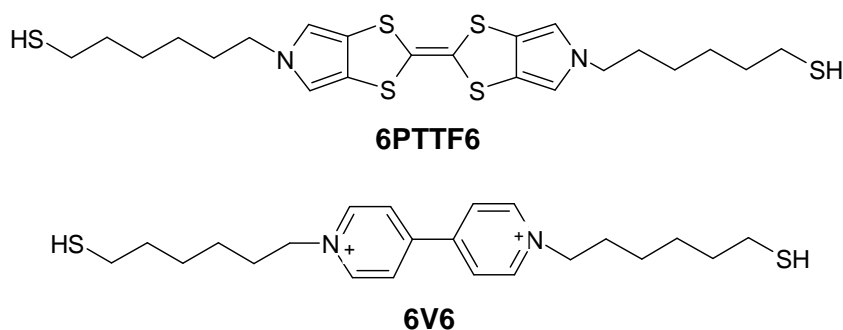


**Figure 5.5:** Molecular structure of 6PTTF6 and 6V6.<sup>20, 23</sup>

The pyrrolo-tetrathiafulvalene (6PTTF6), an electron rich compound that is planar in structure in both the neutral and monocation states, is linked between a gold substrate and tip via an alkane thiol chain. The two reversible oxidation processes reported for TTF compounds<sup>6</sup> are observed for 6PTTF6 and they fall within a potential range in which the Au-S bonds are stable in aqueous electrolyte. The viologen ring, which also has two redox states (reducing the dication to the monocation radical and the neutral state), can twist about the central carbon-carbon bond in the dication, depending on the anion, suggesting that the switch from the planar to the twisted structure is a low energy process.<sup>24</sup> Increased inter-ring carbon-carbon twisting has been observed for a similar viologen salt in the monocation (V<sup>+</sup>) state indicating large configurational differences between the dication and singly reduced monocation.<sup>25</sup> These structural fluctuations may explain the differences in conductance between the 6PTTF6 and 6V6 compounds in that the tunnelling factor depends on the nuclear configuration of the twisting mode of the viologen whereas the planar mode observed for the 6PTTF6 system allows for a different current/overpotential relation resulting in the “off-on-off” switching mode.

6PTTF6 is linked to the Au electrode and STM tip via alkane thiol chains at either end with the TTF unit in the centre. DipyrBEDT-TTF (**D**, Table 5.1), discussed in this chapter, allows for a smaller distance between the redox sites of the TTF unit and the electrode with binding occurring through two pyridine linkers. In 2004 Lindsay *et al.*<sup>26</sup> reported the self assembly of a TTF derivative that binds directly to a Au(III) surface via a S-Au bond in which the monolayers are disordered and pack in lateral dimensions with alkyl chains flowing from the other end of the TTF core, Figure 5.6. This compound is proposed as a suitable candidate for a “molecular wire”.

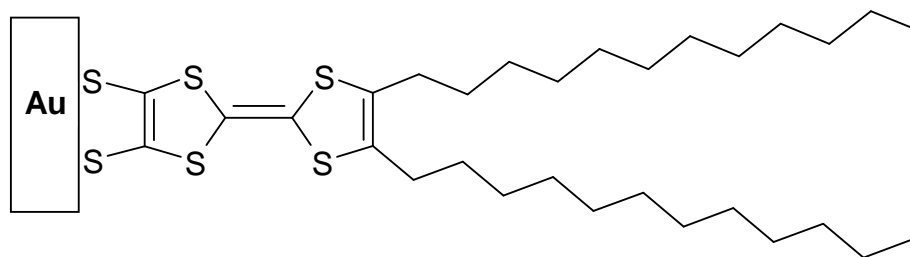


**Figure 5.6:** Molecular structure of a TTF derivative self assembled on a Au(III) surface.<sup>26</sup>

STM images of this compound show a high density of defects in the monolayer resulting from the disordered fashion in which they assemble. Terraces that are as deep as a single gold atom are observed as well as pit-like defects. The alkyl chains have freedom to move (being referred to as fluid-like and non-uniform) and the lack of lateral interaction between them means the resulting monolayer is not dense. The resistance of this TTF derivative was measured and compared with two other “molecular wires”. The first of these was the conjugated carotenedithiol<sup>27</sup> that is almost as long as the TTF molecule in Figure 5.6 with 28 carbon atoms, and the second comparison is made with the 2,5-di(phenylethynyl-4'-thioacetyl)benzene (TPE)<sup>28</sup> with measured resistances of  $4.9 \pm 0.2$  and  $52 \pm 18$  G $\Omega$  respectively. The resistance of the TTF molecule, measured as  $25.7 \pm 0.3$  G $\Omega$  using a metal coated conducting atomic force microscope (c-AFM), falls between these two values despite its length being similar to the carotenedithiol molecule. This suggests that the positioning of the TTF core so close to the surface of the electrode and the non-perpendicular packing of the monolayer relative to the surface are important aspects in

mediating a large conductance in the molecule; it is postulated that the metal coated c-AFM tip may be almost in direct contact with the bulk of the redox active TTF unit.

#### 5.1.4 Self-Assembled Monolayers of TTF Derivatives

The self-assembly of TTF derivatives on metal electrodes (Pt and Au) have been reported.<sup>29, 30, 31, 32</sup> In 1994, Yip and Ward<sup>30</sup> presented the formation of monolayer charge transfer complexes, containing a TTF based molecule and TCNQ, immobilised on a surface. The 16-mercaptohexadecyl tetrathiafulvalene carboxylate compound binds to a Au electrode via the pendant thiol group rather than through the TTF core, Figure 5.7.

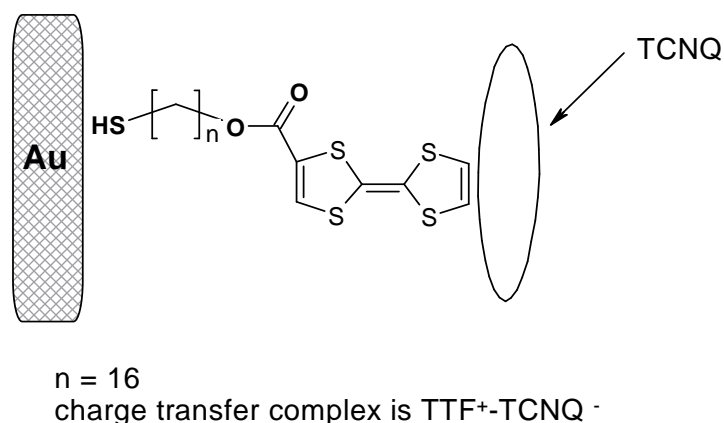
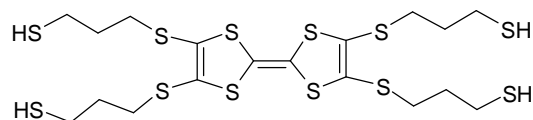
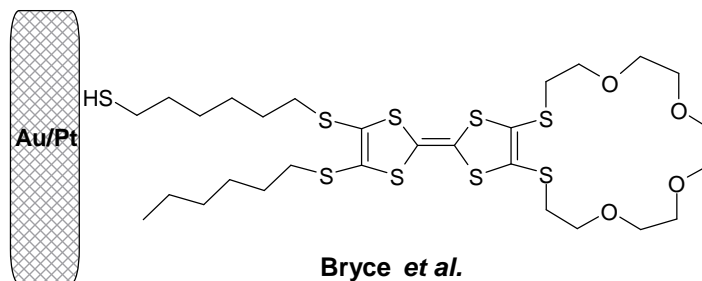


**Figure 5.7:** Illustration of the monolayer charge transfer complex immobilised on Au as reported by Yip and Ward.<sup>30</sup>

The electrochemical response from the monolayer is very similar to that of the free complex in solution with two voltammetric waves characteristic of the TTF core observed. Oxidising both redox centres to form the dication with repeated electrochemical cycling of the TTF monolayer, resulted in diminishing current intensities which suggests that the fully oxidised monolayer is not chemically stable on Au. Introduction of the TCNQ molecule leads to the immobilised charge transfer complex,  $\text{TTF}^+\text{TCNQ}^-$ , in which the  $\text{TCNQ}^-$  anion is oriented in a manner where it is parallel to the surface.<sup>30</sup>



Fujihara *et al.*



Bryce *et al.*

**Figure 5.8:** TTF derivatives reported to form monolayers on Au and Pt via self-assembly where the alkane-thiol chains act as the linker groups.<sup>31, 32</sup>

Fujihara *et al.*<sup>31</sup> reported the self-assembly and electropolymerisation of alkane-thiol functionalised TTF compounds on Au and glassy carbon electrodes respectively. The resulting monolayer of the tetrathiol TTF-derivative (Figure 5.8 (top)), through electrochemical cycling, has shown to be more stable than the monothiol TTF-derivative. The tetrathiol TTF compound also forms stable multilayers via electropolymerisation.

Self-assembly of S<sub>2</sub>O<sub>4</sub>-crown annelated tetrathiafulvalene derivatives on Pt and Au electrodes have been reported by Bryce *et al.*<sup>32</sup> where binding to the electrode surface occurs through a terminal alkane-thiol chain, Figure 5.8 (bottom). The monolayers exhibit an electrochemical response characteristic of the TTF core and a linear relationship between the peak current and scan rate is observed. The monolayers exhibit limited stability in aqueous electrolyte when oxidising to the dication. However, much greater stability is noted when oxidation is restricted to the formation of the monocation radical only. Adsorption of the monolayer on Pt gives a more reproducible electrochemical response than that formed on Au. The crown ether acts as an ionophore in acetonitrile allowing metal complexation with cations such as K<sup>+</sup>, Na<sup>+</sup>, Ba<sup>+</sup> and Ag<sup>+</sup>. The occurrence of metal complexation with the TTF compound was determined through positive shifts of the first oxidation potential.<sup>32</sup>

This chapter contains the study of a pyridine substituted BEDT-TTF analogue, 5,6 – dehydro-5,6-di(pyrid-4-yl)-bis(ethylenedithio)tetrathiafulvalene (compound **D** in Table 5.1), referred to as dipyrBEDT-TTF for short, the synthesis of which was carried out within the Prof. John D. Wallis research group in Nottingham Trent University, UK.<sup>15a</sup> In the case of this compound, and as opposed to the D- $\sigma$ -A approach above, an alternative method is considered for investigating its potential use as a molecular component in electronic devices where the conductivity in the molecule is measured as a function of the redox states within. The solution-phase diffusion controlled electrochemistry and spectroelectrochemistry as well as monolayer formation of dipyrBEDT-TTF are discussed. The effects of different solvents on the diffusion controlled oxidation potentials are examined. The electrochemical properties of both the solution-phase and monolayer are characterised using cyclic voltammetry in the presence and absence of oxygen.

## 5.2 Results and Discussion

### 5.2.1 Redox Properties

#### 5.2.1.1 Solution Phase Diffusion Controlled Electrochemistry

The redox chemistry of TTF and its derivatives is well documented in the literature.<sup>2, 6, 8</sup> In general for TTF and BEDT-TTF compounds, cyclic voltammetry reveals two reversible anodic redox waves: the first of these corresponds to the oxidation of the neutral species forming the stable monocation radical. At higher potentials the formation of the dication is observed upon the second oxidation of the TTF core. These processes occur within a readily accessible potential range forming stable redox states.

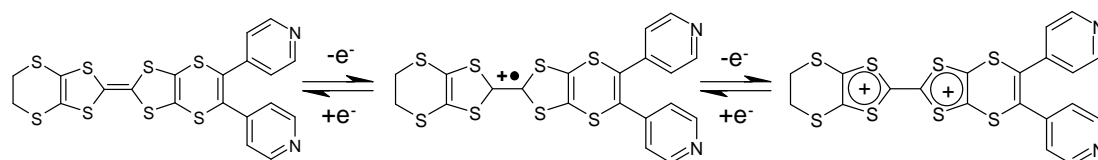


**Figure 5.9:** Transformation of the neutral dipyrBEDT-TTF to the dication through the stable monocation redox state.

The oxidation potentials of TTF are sensitive to the electron donating/withdrawing properties of substituents on the dithiole rings. Evidence of this lies in the comparison of TTF and BEDT-TTF redox potentials, Table 5.1. The electron withdrawing ethylenedithio groups of the latter stabilise the HOMO levels of the TTF core and an increase in the oxidation potentials of the compound is observed. This is further supported by comparing the redox potentials of TTF with those of the first  $\pi$ -extended dibenzo TTF derivative, reported in the literature in the first half of the 20<sup>th</sup> century by Hurlley *et al.*<sup>33, 6</sup> half a century before that of the unsubstituted TTF molecule. The oxidation potentials of the latter are 260 and 270 mV more positive for the first and second oxidation potentials respectively as a result of the extended  $\pi$ -conjugating from the benzene rings. The solution phase diffusion-controlled electrochemistry of dipyrBEDT-TTF was measured using cyclic voltammetry (CV) and differential pulse voltammetry (DPV). Two redox waves typical of the TTF unit are observed

representing the oxidation to the monocation radical and subsequent dication species, Figure 5.10.

Wallis and Almeida *et al.*<sup>15a</sup> reported the diffusion-controlled redox potentials of dipyrBEDT-TTF as +0.75 and +1.07 V (vs. Ag/AgCl), for the first and second oxidations respectively. In this chapter the half-wave potentials ( $E_{1/2}$ ) were recorded at +0.64 and +0.97 V (on a platinum working electrode) for the corresponding processes in dichloromethane with 0.1 M tetrabutylammonium hexafluorophosphate as the supporting electrolyte, Figure 5.10.

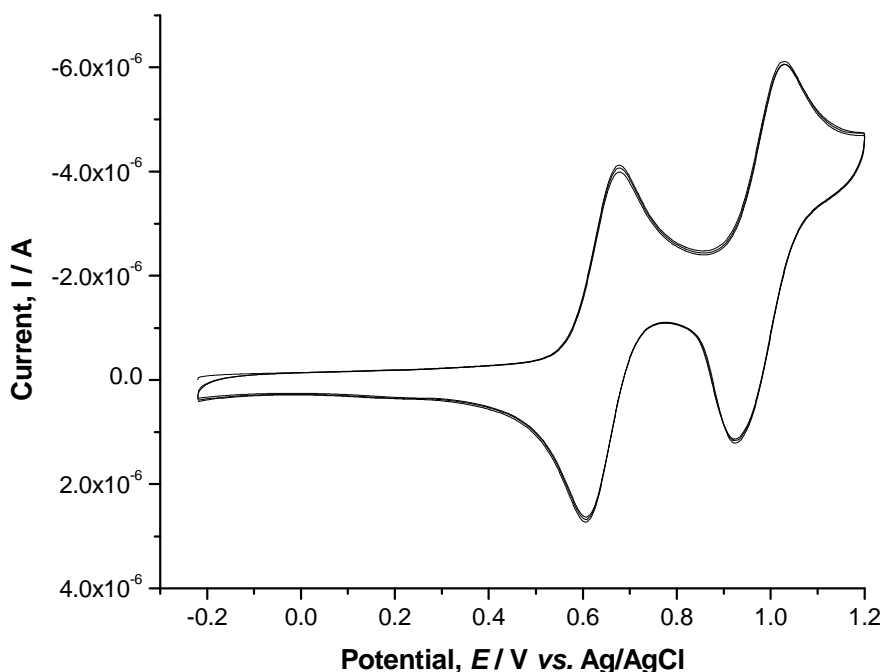


**Figure 5.10:** Cyclic voltammogram of the anodic processes of dipyrBEDT-TTF [C: 1mM], at a platinum working electrode (real surface area =  $0.0818 \text{ cm}^2$ ), vs. Ag/AgCl, in dichloromethane with 0.1 M TBAPF<sub>6</sub> as the supporting electrolyte. Scan rate: 100 mV/s.

Scanning toward negative potentials, in solution phase diffusion-controlled cyclic voltammetry of dipyrBEDT-TTF, to a potential of -2.0 V reveals two cathodic waves ( $E_{pc} = -1.43$  and  $-1.82$  V, vs. Ag/AgCl) representing two irreversible processes. TTF compounds exhibit strong  $\pi$ -donor properties. As such there are few reports in the

literature of the reduction potentials of the TTF component of these types of complexes. This is most likely due to large negative reduction potentials for the TTF core given its electron rich character. Reduction potentials have been reported by Shen *et al.*<sup>34</sup> for perylene substituted TTF derivatives and by Martín and Seoane *et al.*<sup>35</sup> for benzoquinone substituted TTF dyads. In both cases reduction of the complex is assigned as being located on the perylene and benzoquinone moieties and not the TTF core itself. The cathodic processes observed for dipyrBEDT-TTF (Figure 5.11), therefore may be assigned as the reduction of each pyridine ring, and not the central TTF unit, forming anion radicals on each ring.<sup>36</sup>

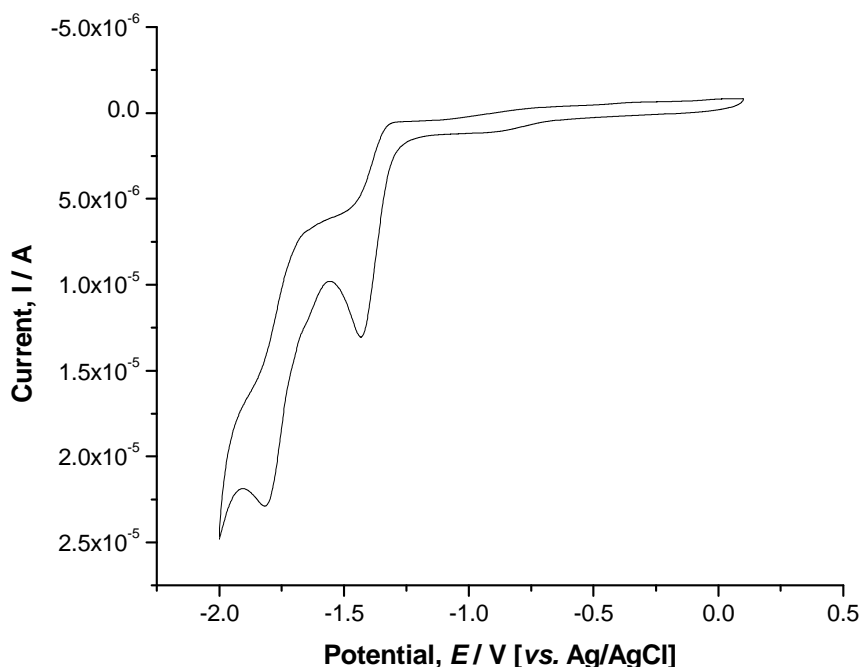


**Figure 5.11:** Cyclic voltammogram of the cathodic processes of dipyrBEDT-TTF [C: 1mM], at a platinum working electrode (real surface area =  $0.0818 \text{ cm}^2$ ), vs. Ag/AgCl, in dichloromethane with 0.1 M TBAPF<sub>6</sub> as the supporting electrolyte. Scan rate: 100 mV/s.

In order to be classed as a reversible redox process the cyclic voltammetric waves must possess certain characteristic features. The Nernst equation (Chapter 2) is used to relate the measured potential to the concentration of the redox active species involved in the electrode process. Systems that obey this equation are said to be

electrochemically reversible.<sup>37, 38</sup> The separation between the anodic and cathodic peaks of a redox process,  $\Delta E_p$ , can be calculated by subtracting the cathodic peak potential from the anodic peak potential (Equation 2.15, Chapter 2). Formally this value should equal 59 mV for a one-electron process at 25° Celsius, as found from the Nernst equation.<sup>37</sup> Under experimental conditions values of between 60 – 100 mV are generally accepted for a reversible redox process and the values for  $\Delta E_p$  obtained for dipyrBEDT-TTF are within the range of 60 – 100 mV, Table 5.2. For a reversible process, the ratio of the anodic and cathodic peak currents should be equal to unity. The values calculated for dipyrBEDT-TTF, although not exactly equal to one, are within close range.

Electrode	$E_{1/2}$ [V], 1 <sup>st</sup> Oxidation ( $E_{pa} - E_{pc}$ , mV)	$E_{1/2}$ [V], 2 <sup>nd</sup> Oxidation ( $E_{pa} - E_{pa}$ , mV)	$\Delta E$ [mV]	$i_{pa} : i_{pc}$ , 1 <sup>st</sup> Oxidation	$i_{pa} : i_{pc}$ , 2 <sup>nd</sup> Oxidation
Platinum	+0.64 (70)	+0.97 (100)	330	1.01	1.19

**Table 5.2:** Diffusion-controlled data for the reversible anodic processes of dipyrBEDT-TTF at a Pt working electrode, vs. Ag/AgCl, in dichloromethane with 0.1 M TBAPF<sub>6</sub> as the supporting electrolyte. Scan rate: 0.1 V/s.

For fully reversible systems, a plot of the peak potential,  $E_p$  versus the scan rate,  $v$  will show that two parameters are independent of each other. Table 5.3 outlines the observed changes in  $E_p$  as a function of scan rate. Minor fluctuations are observed for scan rates ranging from +0.1 to +1.0 V/s, Figure 5.12.  $\Delta E_p$  also exhibits changes of only 10 mV when the scan rate is varied. However, stepping beyond the range of 1.0 v/s and scanning at rates as high as 7.5 V/s results in the observation of positive shifts of up to 60 mV and 70 mV for the first and second redox waves respectively. This can suggest that kinetic limitations exist for the electron transfer and each process may be deemed as *quasireversible*.<sup>37, 39</sup> This observation is in contrast to the results outlined in Table 5.2 where the differences in anodic and cathodic peak potentials, as well as the ratio of the anodic and cathodic peak currents are within the range of those values outlined for a reversible system. However, at higher scan rates the increase in current

results in an increase in the  $iR$  drop between the working and reference electrodes which can result in shifts in the peak potentials of the redox process.

$\nu$ (V/s)	1 <sup>st</sup> Redox Process		2 <sup>nd</sup> Redox Process		$\Delta E_p$ (mV)
	$E_{pa}$ (V)	$E_{pc}$ (V)	$E_{pa}$ (V)	$E_{pc}$ (V)	
0.5	+0.67	+0.58	+1.02	+0.88	350
0.75	+0.68	+0.58	+1.02	+0.88	340
1.0	+0.68	+0.57	+1.03	+0.87	350
5.0	+0.72	+0.53	+1.07	+0.86	350
7.5	+0.73	+0.52	+1.09	+0.85	360

**Table 5.3:** Cyclic voltammetric data for the relationship between the scan rate,  $\nu$ , and the anodic peak potential,  $E_{pa}$ , of the first and second redox waves in dipyrBEDT-TTF. The data was obtained using a Pt working electrode in dichloromethane vs. Ag/AgCl reference electrode.

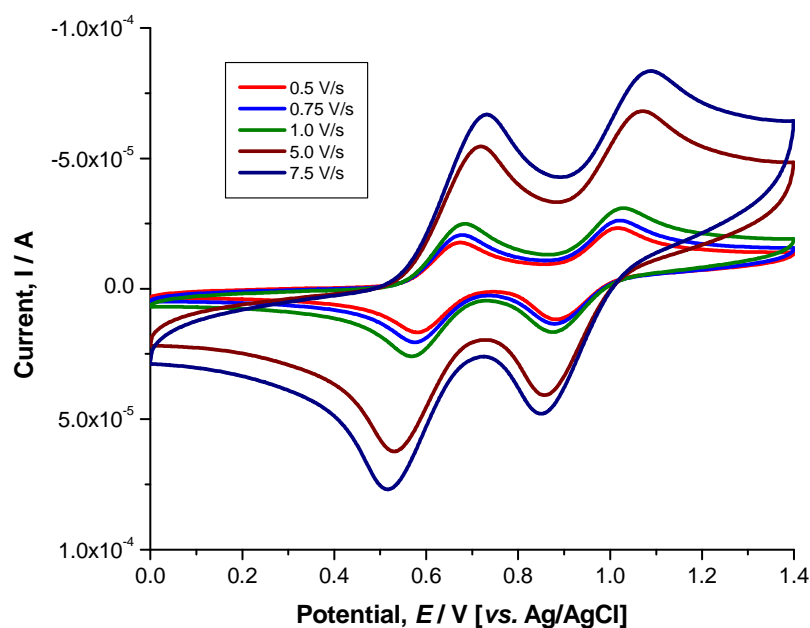


**Figure 5.12:** Scan rate dependence of the diffusion controlled dipyr-BEDT-TTF at a Pt working electrode, vs. Ag/AgCl, in dichloromethane using 0.1 M TBAPF<sub>6</sub> as the supporting electrolyte.

Another method for ascertaining the reversibility of a redox process is evaluating the relationship between the scan rate and the measured peak current. In the case of a diffusion controlled processes a linear relationship exists between the square root of the scan rate and the current for a reversible process.

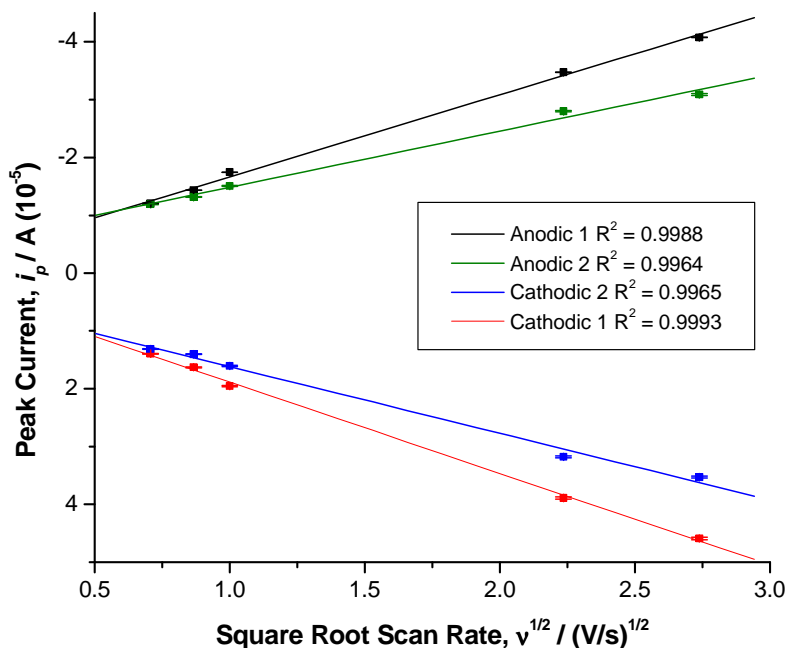


**Figure 5.13:** Graph of the relationship between the square root of the scan rate and the peak currents for the diffusion controlled cyclic voltammetry of dipyrBEDT-TTF in dichloromethane at a Pt working electrode. Anodic 1 and cathodic 1 represent the two waves of the less positive redox process with anodic 2 and cathodic 2 representing the 2<sup>nd</sup> redox process.

Figure 5.13 presents a linear relationship between the peak current and  $v^{1/2}$ . This plot along with the values calculated for  $\Delta E_p$  and the ratio of the peak currents suggests that both of these anodic redox processes on the TTF core of dipyrBEDT-TTF are reversible in nature. It also suggests that the deviations in the oxidation potentials observed during the scan rate dependence experiment arise as a result of an increase in the uncompensated resistance between the reference and working electrodes and a consequent increase in the associated  $iR$  drop.

### 5.2.1.2 Solvent Dependence Study

Within electrochemical cells a medium must always be present through which an electrochemical reaction can take place. The anions and cations from the electrolyte provide a means of conductivity to and from the electrodes through the solvent. For electrochemical experiments there is no one solvent that is suited to all. The choice of solvent for the electrolyte can heavily depend on the electroactive species' solubility properties.

The solvating ability is another property that is considered with electrochemical solvents. It is often required that the solvent solvates the reactant and/or products in an electrochemical reaction. Knowing the potential range of the electrolyte solvent is critical as electrodes are often scanned to, and held at particularly high potentials which may be in the range of the oxidising or reducing potential of the solvent. Other factors such as polarity, dielectric constant and acidity/basicity of a solvent can also influence the electrochemistry of the electroactive species. In this section the electrochemistry of dipyrBEDT-TTF in four different solvents is examined. These include the polar aprotic solvents dichloromethane ( $\text{CH}_2\text{Cl}_2$ ), tetrahydrofuran (THF), acetone and dimethylformamide (DMF).

The different properties of solvents, as well as the nature of the electrolyte, have been shown to influence the redox properties of molecules in an electrochemical environment including the reversibility and rates of reaction.<sup>40</sup> The effect of the solvent on the potentials of the first and second redox processes, and the stability of the monocation intermediate ( $\Delta E$ ), has been investigated. The redox potentials of the dipyrBEDT-TTF in each solvent are given in Table 5.4 below. Solvent properties such as polarity, dielectric constant and Lewis basicity/acidity (Gutmann donor/acceptor numbers)<sup>41</sup> have been considered.

In order to define polarity in the context of chemical systems the degree of separation of electronic charge within a molecule must be considered. This separation of charge results in the formation of an electric dipole, i.e. the existence of separate positive and negative charges. In molecules where the electronegativity of one atom is greater than another a situation results where the electron density is shared unequally between the two sites. The molecule may be termed 'polar' with  $\text{H}_2\text{O}$  being the simplest of

examples. In the alternative case where the electron density is equally shared, a ‘non-polar’ molecule results, e.g. methane, CH<sub>4</sub>.<sup>42</sup>

Solvent	$E_{1/2}$ (V) 1 <sup>st</sup> Redox Wave [ $\Delta E_p$ (mV)]	$E_{1/2}$ (V) 2 <sup>nd</sup> Redox Wave [ $\Delta E_p$ (mV)]	$\Delta E$ (mV)
Dichloromethane	+0.64 [70]	+0.97 [100]	330
Tetrahydrofuran	+0.76 [90]	+0.86 [65]	100
Acetone	+0.66 [70]	+0.82 [75]	160
Dimethylformamide	+0.72 [60]	+0.81 [50]	90

**Table 5.4:** Electrochemical data for the diffusion controlled processes of dipyrBEDT-TTF in different solvents under anaerobic conditions, recorded at a Pt macro working electrode. All potentials have been corrected against the Ag/AgCl reference electrode.

The change in redox potential, with increasing polarity of the electrochemical solvent, for the first and second anodic processes of dipyrBEDT-TTF, as well as the effect on the peak to peak separation ( $\Delta E$ ) between these two waves, has been examined.

It is safe to conclude that there is no relationship between the first oxidation potential and the polarity of the solvent, Table 5.5. The lack of a trend between  $\Delta E$  and polarity is also noted. There is however, a slight inverse proportionality observed between the redox potential of the second wave with that of the polarity: as the polarity of the solvent increases the redox potential of this second, more positive wave decreases - although a lack of linearity in this relationship is noted.

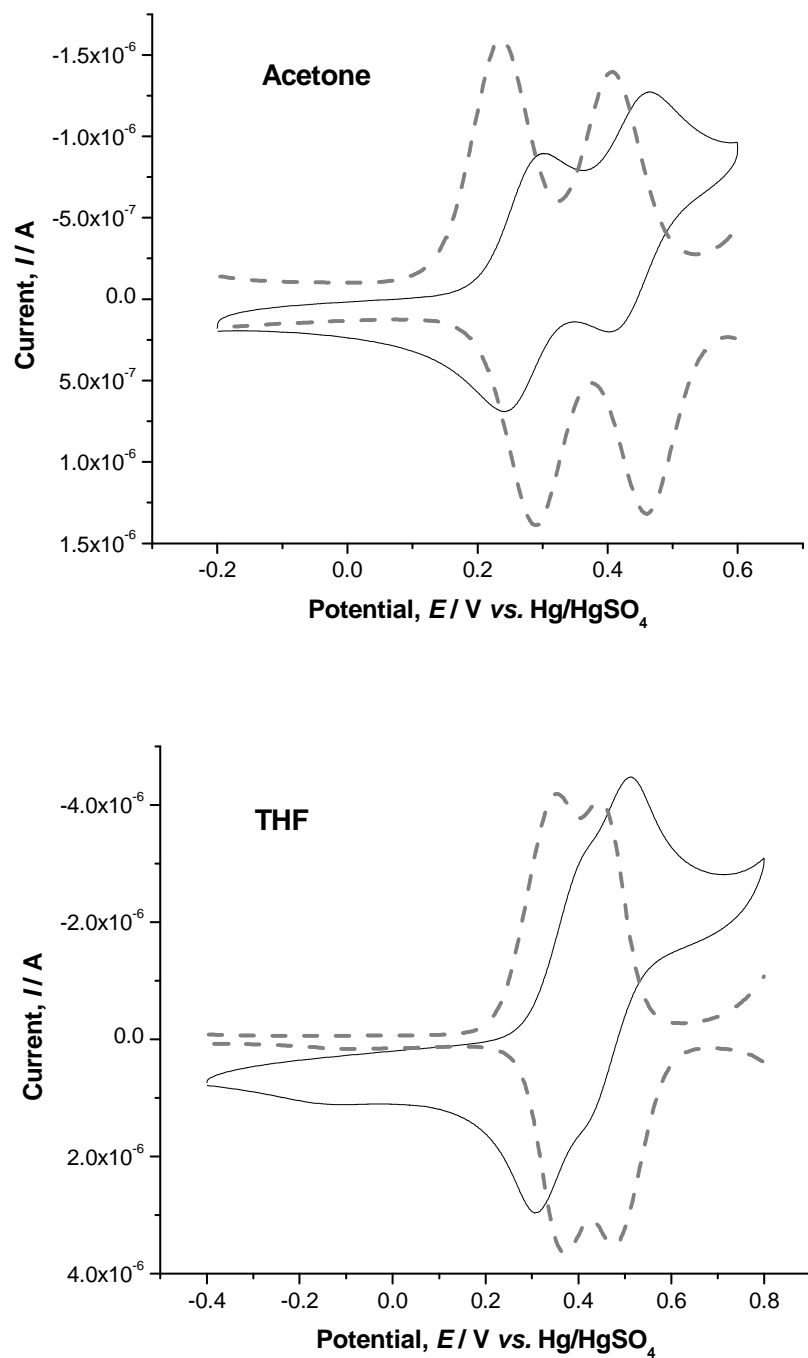


**Figure 5.14:** Cyclic voltammograms (solid line) and differential pulse (dashed line) of dipyrBEDT-TTF [1mM], on a platinum working electrode, vs. Hg/HgSO<sub>4</sub>, in acetone (top) and THF (bottom) with 0.1 M TBA PF<sub>6</sub> as the supporting electrolyte. Scan rate: 100 mV/s.

The dielectric constant of a solvent is a measure of the extent at which a material can conduct electricity when placed in an electric field. This property also indicates the

solvents ability to reduce the strength of an electric field surrounding a charged particle in the solvent. The dielectric constant of a solvent is related to its polarity to a certain extent. Solvents with dielectric constants lower than 25 can be considered ‘non-polar’ whereas those that have values higher than this are polar solvents.<sup>38</sup> Solvents with high dielectric constants allow for greater dissociation of ionic solutes leading to lower solution resistance. This is an important factor in electrochemical experiments. The observed changes in the redox chemistry of dipyrBEDT-TTF were compared with changes in the dielectric constants of the electrochemical solvents. However, no trends between these two properties appear.

Solvent	$\Delta E$ (mV)	Polarity Index <sup>43</sup>	Dielectric Constant ( $\epsilon$ ) <sup>44</sup>	Gutmann Acceptor Number (AN)	Gutmann Donor Number (DN)
CH <sub>2</sub> Cl <sub>2</sub>	330	3.1	8.9	20.4	0
Acetone	160	5.1	21.0	12.5	17
THF	100	4.0	7.5	8	20
DMF	90	6.4	38.3	16	26.6

**Table 5.5:** Relationship between the peak to peak separation of the first and second redox waves ( $\Delta E$ ) and the different properties of the solvents. All experiments were carried out under the same conditions at a Pt macro working electrode: 0.1 M TBAPF<sub>6</sub> as the supporting electrolyte using argon to achieve an anaerobic atmosphere.

This random behaviour was also observed for the relationship between the electrochemical properties of the molecule and the Gutmann acceptor number.<sup>41</sup> The acceptor number is a measure of the Lewis acidity of a solvent. That is, its ability to accept a pair of electrons from the analyte whereas the donor number is a measure of the Lewis basicity (the ability to donate a pair of electrons). The donor and acceptor numbers of solvents were proposed by Viktor Gutmann in 1976. They are measured using nuclear magnetic resonance spectroscopy (NMR) focusing on the triethylphosphine oxide chemical shift where SbCl<sub>5</sub> is used as the internal standard.<sup>45</sup>

The solvent dependence of the redox properties of dipyrBEDT-TTF are outlined in Table 5.5. With respect to the solvent donor number it is evident that the first redox potential is predominantly solvent independent. This behaviour is also observed for other properties associated with the solvent like the acceptor number, polarity and dielectric constant where no clear trend was observed. However, it is noted that the distance  $\Delta E_p$  (mV) between the first and second redox waves is sensitive to changes in the solvent-electrolyte medium. A trend has been observed between the donor number of the solvent and  $\Delta E_p$ . As the donor number of the solvent increases the separation between the two waves decreases i.e. they are inversely proportional to one another ( $R^2$  value of 0.98), Figure 5.15.

The donor number describes the solvent's ability to donate a pair of electrons to a species in solution so therefore the higher the Gutmann donor number, the stronger the donating power of the solvent. This ability to donate electron pairs leads to these solvents being classified as having decent nucleophilic character. Radical cations, such as the monocation intermediate of dipyrBEDT-TTF (Figure 5.9), generated by electrochemical oxidation are susceptible to attack by nucleophiles and are therefore generally unstable in highly basic mediums. As the donor strength of the solvent increases, the stability of the intermediate decreases (diminishing  $\Delta E$  as the Lewis basicity increases). The increased donor strengths of solvents such as acetone and DMF make it thermodynamically easier to remove a second electron and oxidise the monocation radical to the dication state. The stability of radical cation intermediates is generally achieved in strongly accepting solvents such as dichloromethane as they exhibit electrophilic character.<sup>38</sup>

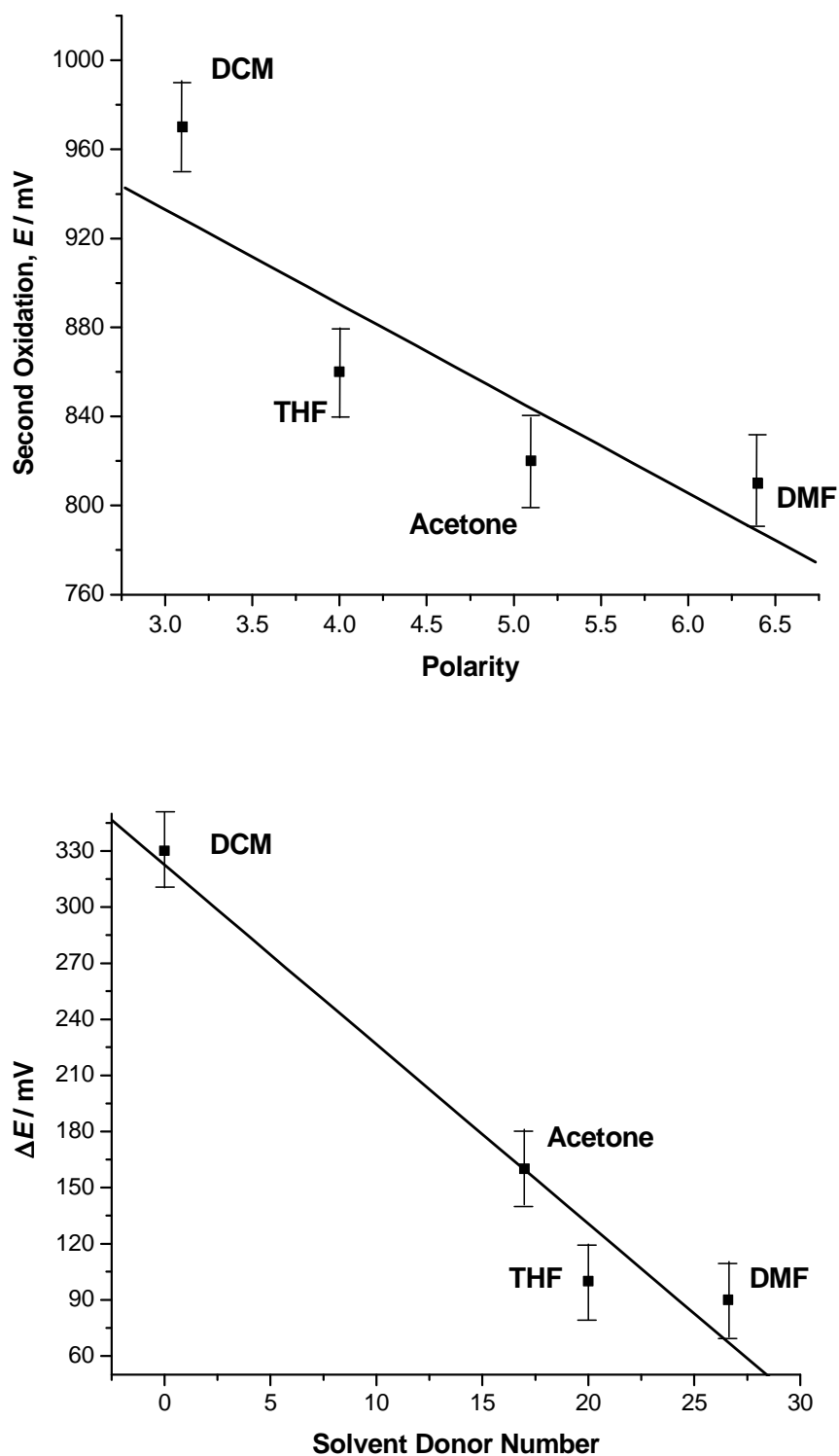


**Figure 5.15:** Graphs to illustrate the relationship between the polarity of the solvent and second oxidation potential of dipyrBEDT-TTF (top) and the solvent donor number with the peak to peak separation,  $\Delta E$ , (bottom). All oxidation potentials referenced against the Ag/AgCl reference.

Without the presence of electrolyte salts in organic solvents the high resistance of the solution prevents a current flowing. Electrochemically inert electrolytes are added to the solvent to induce the flow of the current. The electrolyte will also influence migration of the electroactive species as well as the positive and negative limits of the potential range with participation in ion-pairing with the redox species occurring. The extent to which the solvent-electrolyte system solvates the species in solution depends on the nature of the salt as well as that of the chosen electrochemical solvent.<sup>38</sup>

The influence of ion-pairing between the anions/cations of the electrolyte and the monocation radical in solution was also investigated. Systems where the electrolyte affects the redox species in solution through ion-pairing have been reported for other organic and inorganic systems.<sup>46</sup> TBAPF<sub>6</sub> was the electrolyte chosen for the solvent dependence study. The influence of the anion on the redox chemistry of the dipyrBEDT-TTF molecule was examined through the use of a different anion (perchlorate) using TBA ClO<sub>4</sub> in the electrolyte-solvent medium, Table 5.6.

Electrolyte	$E_{1/2}$ (V) 1 <sup>st</sup> Redox Wave	$E_{1/2}$ (V) 2 <sup>nd</sup> Redox Wave	$\Delta E$ (mV)
TBAPF <sub>6</sub> in CH <sub>2</sub> Cl <sub>2</sub>	+0.64	+0.97	330
TBAClO <sub>4</sub> in CH <sub>2</sub> Cl <sub>2</sub>	+0.72	+0.96	240
TBAPF <sub>6</sub> in Acetone	+0.66	+0.82	160
KPF <sub>6</sub> in Acetone	+0.62	+0.78	160

**Table 5.6:** Electrochemical data for dipyrBEDT-TTF detailing the changes observed with different electrolytes.

From the  $\Delta E$  values recorded for both electrolytes in CH<sub>2</sub>Cl<sub>2</sub> it is clear that the degree of separation between the first and second redox peak is heavily dependent on the nature of the anion component of the electrolyte. The use of the ClO<sub>4</sub><sup>-</sup> anion reduces the value of  $\Delta E$  to 240 mV compared with 330 mV recorded for the PF<sub>6</sub><sup>-</sup> anion. This would suggest that the more compact ClO<sub>4</sub><sup>-</sup> anion decreases the stability of the

monocation radical intermediate and hence a smaller peak to peak separation between the two redox waves is observed.<sup>46a</sup>

Through investigation of the influence of the cationic component of the electrolyte it appears that the observed effect of the electrolyte on the peak to peak separation is confined to the anionic unit of the salt. By using potassium hexafluorophosphate ( $K^+ PF_6^-$ ) as the electrochemical electrolyte instead, the anionic component is unchanged and the effect of the  $K^+$  cation compared to the  $TBA^+$  cation can be investigated. The peak to peak separation remains constant with each different electrolyte (160 mV) thereby indicating that the stability of the monocation radical intermediate of the dipyrBEDT-TTF molecule is controlled by the anionic component of the electrolyte.

### ***5.2.1.3 Aerobic vs. Anaerobic Effects on Stability of the Redox Intermediate***

Electrochemical oxidation of dipyrBEDT-TTF in  $CH_2Cl_2$  reveals two anodic processes involving formation of a cation radical and a dication, Figure 5.10. The stability of the dication species in an aerobic atmosphere was investigated. Through oxidation of the compound over a period of time it was observed that the Faradaic current gradually decreases. This effect was observed with continuous cycling between 0 and +1.20 V (*vs.* Ag/AgCl reference) for approximately three hours. However, after 90 minutes the current observed for the first and second redox processes had completely disappeared, Figure 5.16 (top graph).

The decrease of the Faradaic current was initially observed for the second redox process and, after the current was reduced by approximately 50%, this was followed by a decrease in the observed current of the first redox process. Interestingly, the monocation radical has shown much greater stability in  $CH_2Cl_2$ . By continuously cycling between +0.2 and +0.9 V, *vs.* Ag/AgCl, it is noted that the oxidation of the neutral compound to the redox intermediate does not lead to a decrease in the Faradaic current as was observed for the dication species, Figure 5.16 (bottom). There are several possible reasons for this. The first of which may be the effect of adsorption of the compound of the surface of the Pt electrode which only occurs following the electrochemical formation of the dicationic species.

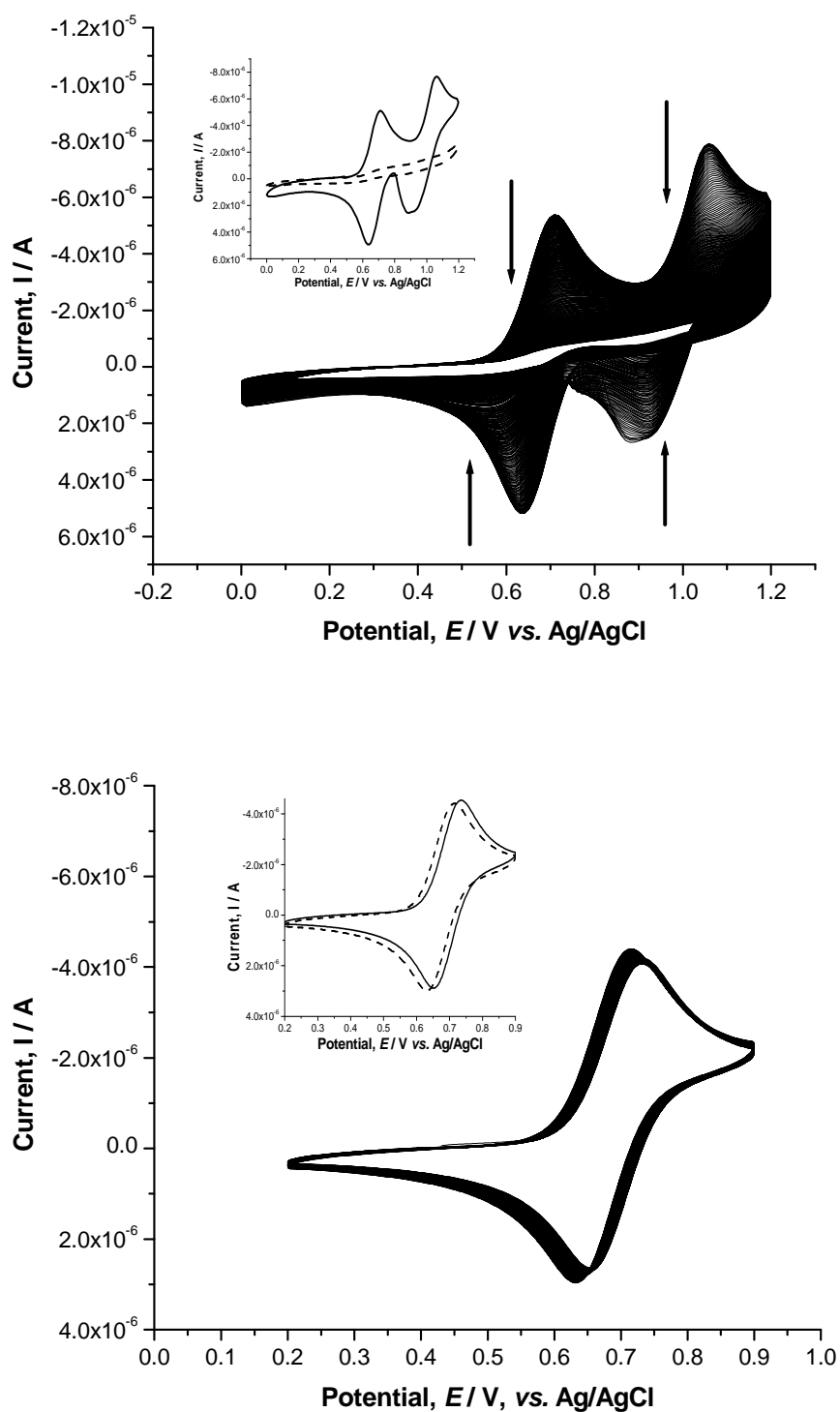


**Figure 5.16:** Cyclic voltammogram of dipyrBEDT-TTF at a Pt electrode in  $\text{CH}_2\text{Cl}_2$  in aerobic conditions with continuous cycling revealing a gradual degradation of the Faradaic current. The top graph shows the dication with the redox intermediate monocation radical presented in the bottom graph. Inset: solid and dashed lines represent the start and end (after 90 minutes cycling) respectively.

Figure 5.17 presents the effects of adsorption of the dicationic form of dipyrBEDT-TTF on a Pt electrode. The working electrode was held at +1.2 V (vs. Ag/AgCl) for a series of quiet times (which is the amount of time the cell is held at the initial potential prior to cycling) ranging from 2 to 240 seconds. After 15 seconds, following oxidation to the dication (indicated by the red line in Figure 5.17) a sharp peak, resembling a desorption “spike” is observed on the return wave which would suggest that the dication species had adsorbed on the electrode surface. The current intensity of the cathodic waves of both processes is greater for the first sweep segment with this returning to that observed when the quiet time was 2 seconds (black line).

Extension of the quiet time to 60 seconds results in a significant decrease in the current with the absence of a desorption peak indicating the formation of a non-conducting layer on the electrode. This trend continues with further decreases observed as the quiet time is increased suggesting that the adsorption of the dicationic species is irreversible at quiet times of 60 seconds and greater.

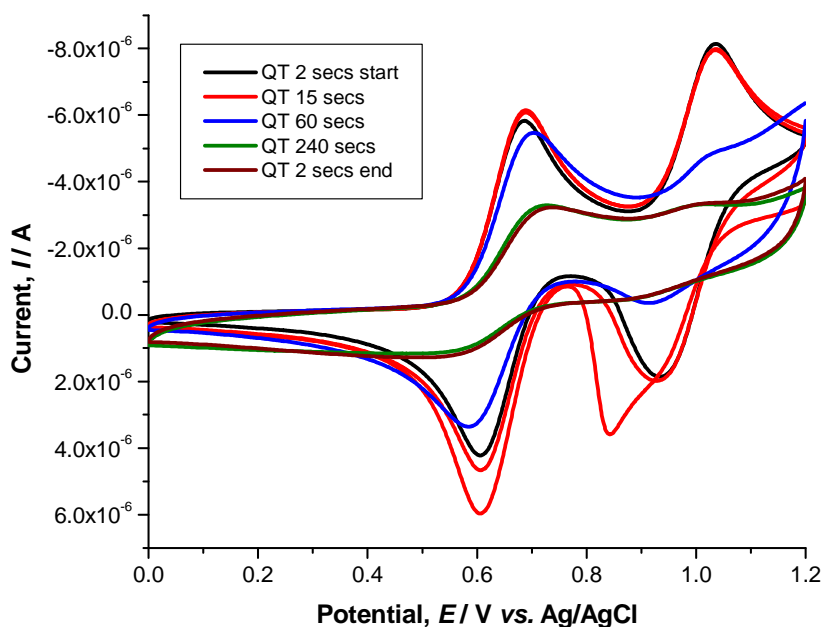


**Figure 5.17:** Adsorption of the dicationic form of dipyrBEDT-TTF at a Pt electrode in dichloromethane under an aerobic atmosphere. Scan rate: 100 mV/s.

Adsorption of the dication of dipyrBEDT-TTF on the electrode surface was considered as a potential reason for the observed degradation of current with continuous cycling over time, Figure 5.16. However, under anaerobic conditions, achieved by degassing using argon, increased stability of the dication was revealed, Figure 5.18. In contrast to the results obtained in an aerobic atmosphere, no reduction of current was observed indicating that the dicationic species does not degrade in the absence of oxygen. The increase in current observed is most likely due to evaporation of the solvent as the cell is kept under a blanket of argon throughout. Adsorption of the dication species on the surface of the electrode is therefore ruled out as a primary reason for the observed decrease in current.

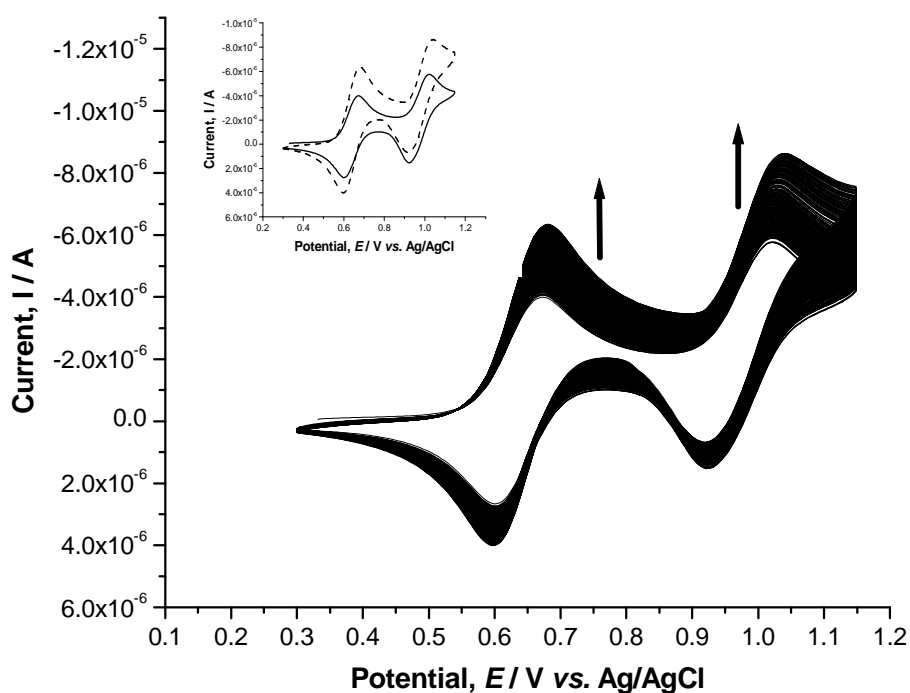


**Figure 5.18:** Solution-phase stability check of dipyrBEDT-TTF at a Pt electrode in  $\text{CH}_2\text{Cl}_2$  in an anaerobic atmosphere with continuous cycling for approximately 80 minutes. Inset: solid and dashed lines represent the start and end respectively. Scan rate: 100 mV/s.

Considering the stability of the monocation radical (Figure 5.16) the degradation of this complex in the presence of oxygen is assumed to arise as a result of a chemical

reaction involving the dication. This reaction is heavily dependent on the presence of molecular oxygen. Molecular oxygen is in the triplet state when in the ground state. Therefore it has two unpaired electrons in its molecular orbitals. Oxidation of the TTF core to the dication results in two positive charges on the molecule. These positive charges are likely to be localised on the sulphur heteroatoms as these are the most electron rich of the TTF core in dipyrBEDT-TTF<sup>2+</sup> and as such are likely to draw the positive charge toward them.

The dication dipyrBEDT-TTF<sup>2+</sup> is stable in an anaerobic environment, i.e. when all the dissolved oxygen has been removed. As such, it is proposed that the proceeding chemical process involves the reactants dipyrBEDT-TTF<sup>2+</sup> and molecular oxygen. Resulting species of this type are well known and reactions between sulphur heterocycles and oxygen have been reported.<sup>47</sup> The possibility of the reaction between dipyrBEDT-TTF<sup>2+</sup> and molecular oxygen leading to a compound with a sulfoxide or sulfone functionality is considered however the exact nature of this species is, as of yet, unknown.

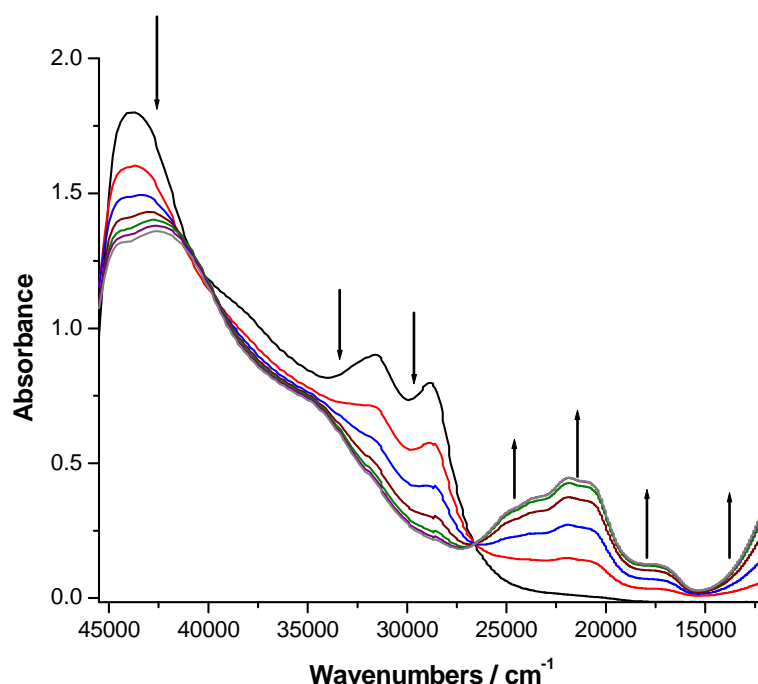
## 5.2.2 Oxidative Spectroelectrochemistry

The stability of the singly oxidised monocation radical of dipyrBEDT-TTF was also investigated using spectroelectrochemistry where the monocation species was generated electrochemically with the induced changes monitored using absorbance spectroscopy. The absorbance bands of the neutral, and monocation radical, form of dipyrBEDT-TTF are presented here and these values are compared with those reported for the neutral, and monocation radical form of BEDT-TTF, Table 5.7.<sup>48</sup>

Compound	Wavelength / nm ± 1 (Wavenumbers / cm <sup>-1</sup> )
BEDT-TTF †	324 (30860), 349 (28650), 466 (21460) <sup>48</sup>
BEDT-TTF <sup>+†</sup>	458 (21830), 486 (20575), 599 (16690), 992 (10080) <sup>48</sup>
dipyrBEDT-TTF	228 (43860), 252 (39680), 316 (31650), 346 (28900)
dipyrBEDT-TTF <sup>+†</sup>	424 (23585), 457 (21880), 479 (20875), 561 (17825), 924 (10820)

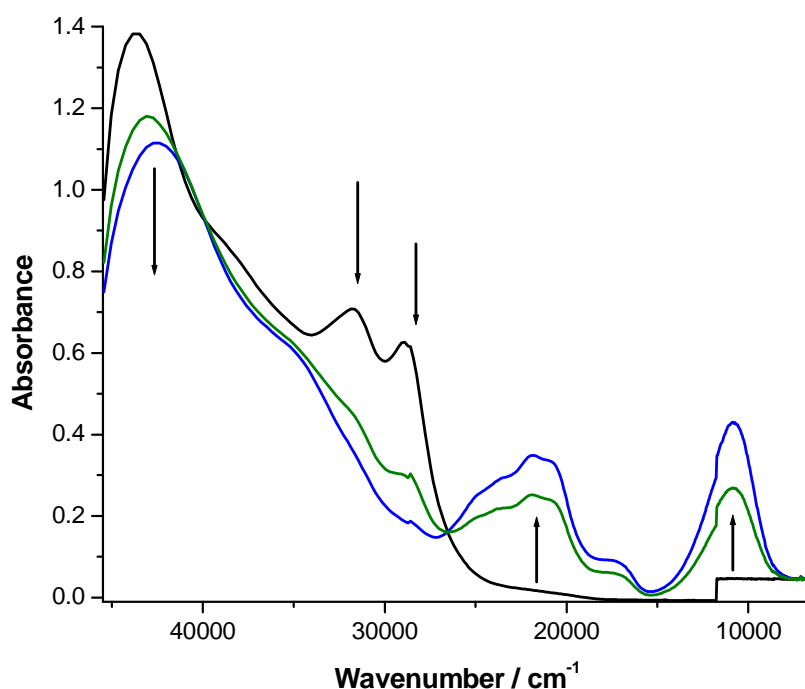
**Table 5.7:** Absorbance data for the neutral and monocation radical forms of dipyrBEDT-TTF (in dichloromethane) and the reference compound BEDT-TTF. Wavenumbers are presented in parentheses. † Recorded in 1,1,2-trichloroethane.<sup>48</sup>

Four absorbance bands are observed in the spectrum of the neutral dipyrBEDT-TTF prior to oxidation. Comparing this data to that reported for a similar compound BEDT-TTF, it is noted that there are two common features in the spectra. The absorbance bands at 31650 and 28900  $\text{cm}^{-1}$  (316 and 346 nm respectively) for dipyrBEDT-TTF are also observed in the absorbance spectrum of BEDT-TTF (324 and 349 nm). Orduna *et al.*<sup>48</sup> proposed that the lower energy bands (349 nm) represent a transition from the HOMO ( $\pi$ ) to the LUMO ( $\sigma^*$ ) with the higher energy wave corresponding to a HOMO to LUMO+1  $\pi \rightarrow \pi^*$  transition. Considering that the absorbance bands at 316 and 346 nm in the spectrum of dipyrBEDT-TTF are close in energy to these bands it may be proposed that they represent similar transitions within the compound. A further two absorbance bands are also exhibited at higher energy than the aforementioned signals in the spectrum of dipyrBEDT-TTF, observed at 43860 and 39680  $\text{cm}^{-1}$  (228 and 252 nm respectively). These bands do not appear in the baseline spectrum and upon oxidation to the monocation radical (*vide infra*) a decrease in the intensity of these bands is observed, Figure 5.19.



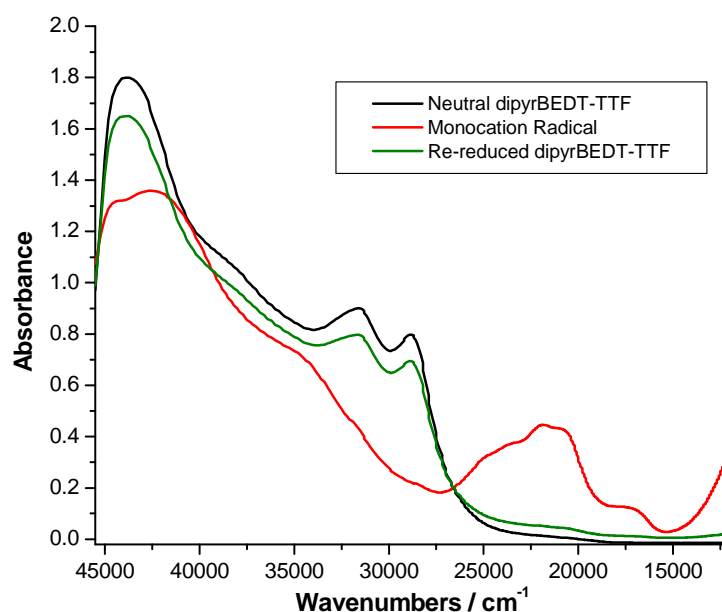
**Figure 5.19:** Spectral variations of the neutral dipyrBEDT-TTF (black line) under controlled electrochemical oxidation ( $E = +0.7$  V, vs. Ag wire) with the conversion to the monocation radical. The spectra were recorded in dichloromethane (0.1 M TBAPF<sub>6</sub>) using a Pt gauze working electrode.

Figure 5.19 reveals the oxidation of dipyrBEDT-TTF. Bulk electrolysis at +0.7 V (vs. Ag wire), a potential approximately half way between the potentials of the first and second redox species, allows for conversion to the monocation radical without further oxidation to the dication species. This process is represented in the absorbance spectra by a decrease in the bands at 43860, 31650 and 28900  $\text{cm}^{-1}$  (228, 316 and 346 nm respectively) with the appearance and concomitant increase in new absorbance bands at 23585, 21880, 20875, 17825 and 10820  $\text{cm}^{-1}$  (424, 457, 479, 561 and 924 nm). The high intensity, lowest energy transition is only observed when the wavelength is extended into the Near-IR region, Figure 5.20. There are similarities between the energies of these new transitions and those of the monocation radical of BEDT-TTF, Table 5.7. The lowest energy absorbance band observed for the  $\text{BEDT-TTF}^+$  is reported to represent the transition of charge from the HOMO of the monocation radical to the SOMO which is created upon oxidation of the neutral species.<sup>48</sup>



**Figure 5.20:** Spectral variations of the neutral dipyrBEDT-TTF (black line) under controlled electrochemical oxidation in dichloromethane (0.1 M  $\text{TBAPF}_6$ ) using a Pt gauze working electrode. Black line: neutral species. Green and blue lines: Oxidation to monocation radical,  $E = +0.7$  V.

An isosbestic point is observed in the absorbance spectra at 376 nm, Figure 5.19 to Figure 5.21. At this wavelength in the spectrum the molar absorptivity of both the neutral dipyrBEDT-TTF and the monocation radical, dipyrBEDT-TTF<sup>+</sup> are equal. Conversion from the neutral species to the monocation radical is a direct reaction with no intermediates or side products and the rate of change of oxidation of the neutral compound to the monocation radical is linear.



**Figure 5.21:** Spectral variations of dipyrBEDT-TTF under controlled electrochemical oxidation using a Pt gauze working electrode in dichloromethane (0.1 M TBAPF<sub>6</sub>). Black line: neutral species. Red line: dipyrBEDT-TTF<sup>+</sup>,  $E = +0.7$  V. Green line: re-reduced species,  $E = +0.2$  V.

Electrochemical results indicate that the oxidation of dipyrBEDT-TTF to the monocation radical, dipyrBEDT-TTF<sup>+</sup> is a reversible process and that this redox intermediate is stable in both aerobic and anaerobic conditions, Figure 5.16. The neutral species is oxidised, via bulk electrolysis at a potential of +0.7 V (vs. Ag wire), to the dipyrBEDT-TTF<sup>+</sup> and spectral variations corresponding to the formation of this radical species are observed, Figure 5.19. Changing the potential to +0.2 V allows for reduction of this monocation radical back to the neutral species. The observed changes

in the absorbance spectrum that arise as a result indicate that this oxidation is in fact reversible and the monocation radical species is stable as the final spectrum has the same features as those observed in the original spectrum, Figure 5.21.

### 5.2.3 Comproportionation Constant, $K_c$

In the design of a molecular system for use as a molecular diode in electronic devices, one must consider the redox chemistry of the compound as well as the communication between the redox centres - an advantage in the realisation of rectifying behaviour within molecules. Spectroelectrochemistry is a valuable technique in the investigation of electronic interaction between redox centres in a molecule. This technique was used in Chapter four to examine the intramolecular interaction between the metal centres across the bridging ligand: identified by the presence of intervalence charge transfer bands in the spectrum of the mixed valence state which were no longer visible when the complexes were fully oxidised. Unfortunately, dipyrBEDT-TTF exhibits poor stability when oxidised to the dication in an aerobic environment. As the spectroelectrochemical experiments discussed in this thesis were performed in the presence of oxygen it was not possible to determine whether the absorbance bands visible in the spectrum of the monocation radical were those of intervalence bands or simply intramolecular charge transfer bands.

However, electrochemical results obtained from cyclic voltammetry can be used as an indicator of the stability of the monocation radical redox intermediate and the possible presence of electronic coupling between the redox centres in the molecule. The simultaneous oxidation of two redox centres within a molecule, and hence the presence of only one anodic wave in the cyclic voltammogram, usually indicates the absence of electronic coupling between the centres. The observation of two distinct redox waves in a CV denotes that a mixed valence species may have formed following oxidation of the first redox centre.<sup>49</sup> The comproportionation constant  $K_c$ , as defined in Chapter 4, is a measure of the stability of the redox intermediate intervalence compound. This is defined in equation 4.8 of Chapter 4 for dinuclear transition metal complexes and for the organic dipyrBEDT-TTF may be written as follows:



where R represents a redox centre of dipyrBEDT-TTF and the monocation radical intermediate is defined as  $\text{R}^+\text{R}^0$ .<sup>50</sup>  $K_c$  has been calculated for dipyrBEDT-TTF from the solution-phase diffusion controlled electrochemistry for each of the different solvents, the values of which are given in Table 5.8.

Solvent	$\Delta E$ (mV)	$K_c$
Dichloromethane	330	$3.75 \times 10^5$
Tetrahydrofuran	100	50
Acetone	160	505
Dimethylformamide	90	33

**Table 5.8:** Separation between the first and second redox potentials ( $\Delta E$ ) of dipyrBEDT-TTF and the comproportionation constant,  $K_c$  in different solvents.

The largest values of  $K_c$  were calculated for the compound in dichloromethane and acetone with that of the former being three orders of magnitude greater. The lower values of  $K_c$  stem from the electrochemistry of the dipyrBEDT-TTF in tetrahydrofuran (50) and dimethylformamide (33) where  $\Delta E$  is 100 and 90 mV respectively. These results give an indication of the extent of intervalence interaction between the redox centres within the molecules and suggest that such interaction is most prevalent in dichloromethane. However, relying on electrochemical results alone to determine the extent of interaction is not advised (Chapter 4) and therefore additional spectroelectrochemical measurements in an anaerobic environment are required.

#### 5.2.4 Electrochemical Properties of dipyrBEDT-TTF on a Surface

In addition to the D- $\sigma$ -A approach<sup>8</sup>, rectifier behaviour within molecules has been investigated by measuring the conductivity as a function of the redox states within, where switching between the redox states can be controlled electrochemically.<sup>20, 21</sup> In order to investigate potential rectifier behaviour in molecules with two stable redox states, a monolayer of the compound must first be assembled on the surface of an electrode. In this section the formation of monolayers of dipyrBEDT-TTF are discussed. Both Pt and Au substrates were used in the attempted formation of the monolayer including macro, micro and Au bead electrodes. A series of deposition solvents were used over a range of different concentrations of the compound. Several electrochemical solvents and electrolytes were investigated during the optimisation of the dipyrBEDT-TTF monolayer, Table 5.9.

From the electrochemical results obtained for each experiment outlined in Table 5.9, it is observed that monolayer formation of dipyrBEDT-TTF is sensitive to the nature of the substrate, deposition solvent and electrochemical solvent. Several attempts have been made to assemble the compound on a Au electrode. Au macro, micro and bead electrodes were used, however, the electrochemical response from the monolayer on Au is poor and significantly less than that observed for Pt, Figure 5.22.

Both anodic redox processes, representing the oxidation to the monocation radical and dication are observed in the first CV obtained at a scan rate of 10 V/s (shown in black in Figure 5.22). However, the height of the peak current of the second anodic wave is significantly greater than the peak current observed for the corresponding cathodic wave, as well as the peak currents observed for the first, less positive, redox process. The intensity of this second anodic wave at approximately +0.9 V (vs. Ag/AgCl) decreases with each successive sweep segment.

Deposition Solvent	Concentration of dipyrBEDT-TTF	Electrode	Electrolyte	Electrochemical Solvent
CH <sub>2</sub> Cl <sub>2</sub>	50 μM	Au	0.1 M LiClO <sub>4</sub>	H <sub>2</sub> O
CH <sub>2</sub> Cl <sub>2</sub>	50 μM	Au	0.1 M TBAClO <sub>4</sub>	ACN
CH <sub>2</sub> Cl <sub>2</sub> /ACN (9:1)	50 μM	Au	0.1 M TBAClO <sub>4</sub>	ACN
EtOH	50 μM	Pt	0.1 M TBAClO <sub>4</sub>	ACN
EtOH	50 μM	Pt	0.1 M TBAPF <sub>6</sub>	ACN
EtOH	100 μM	Pt	0.1 M TBAPF <sub>6</sub>	ACN
EtOH	100 μM	Pt	0.1 M TBABF <sub>4</sub>	ACN
EtOH	500 μM	Pt	0.1 M TBAPF <sub>6</sub>	ACN
EtOH/ CH <sub>2</sub> Cl <sub>2</sub> (9:1)	500 μM	Pt	0.1 M TBABF <sub>4</sub>	ACN
EtOH/ CH <sub>2</sub> Cl <sub>2</sub> (7:3)	500 μM	Pt	0.1 M TBABF <sub>4</sub>	ACN
EtOH/ CH <sub>2</sub> Cl <sub>2</sub> (7:3)	1 mM	Pt	0.1 M TBABF <sub>4</sub>	ACN
EtOH/ CH <sub>2</sub> Cl <sub>2</sub> (7:3)	1 mM	Pt	0.1 M TBAPF <sub>6</sub>	ACN
EtOH/ CH <sub>2</sub> Cl <sub>2</sub> (7:3)	1 mM	Pt	0.1 M LiClO <sub>4</sub>	H <sub>2</sub> O
DMF/H <sub>2</sub> O (85:15)	500 μM	Pt	0.1 M TBABF <sub>4</sub>	ACN
DMF/H <sub>2</sub> O (9:1)	500 μM	Pt	0.1 M TBAClO <sub>4</sub>	ACN
DMF/H <sub>2</sub> O (9:1)	1 mM	Pt	0.1 M TBABF <sub>4</sub>	ACN
DMF/H <sub>2</sub> O (9:1)	500 μM	Au Bead	0.1 M TBABF <sub>4</sub>	ACN
DMF/H <sub>2</sub> O (9:1)	500 μM	Au	0.1 M TBAPF <sub>6</sub>	ACN
DMF	500 μM	Au Micro	0.1 M TBABF <sub>4</sub>	ACN
DMF	500 μM	Pt Micro	0.1 M TBABF <sub>4</sub>	ACN
DMF/H <sub>2</sub> O (95:5)	500 μM	Au Micro	0.1 M TBABF <sub>4</sub>	ACN
DMF/H <sub>2</sub> O (95:5)	500 μM	Pt Micro	0.1 M TBABF <sub>4</sub>	ACN
CH <sub>2</sub> Cl <sub>2</sub>	500 μM	Pt	0.1 M TBAClO <sub>4</sub>	ACN
CH <sub>2</sub> Cl <sub>2</sub>	500 μM	Au Bead	0.1 M TBAClO <sub>4</sub>	ACN
CH <sub>2</sub> Cl <sub>2</sub>	500 μM	Pt	0.1 M LiClO <sub>4</sub>	H <sub>2</sub> O
CH <sub>2</sub> Cl <sub>2</sub>	500 μM	Au	0.1 M TBAClO <sub>4</sub>	ACN
CH <sub>2</sub> Cl <sub>2</sub>	500 μM	Pt	0.1 M TBAClO <sub>4</sub>	ACN/H <sub>2</sub> O (90:10)
CH <sub>2</sub> Cl <sub>2</sub>	500 μM	Pt	0.1 M TBAClO <sub>4</sub>	PC †
CH <sub>2</sub> Cl <sub>2</sub>	500 μM	Pt	0.1 M TBAClO <sub>4</sub>	PC/ACN (80:20)
CH <sub>2</sub> Cl <sub>2</sub>	500 μM	Pt	0.1 M TBAClO <sub>4</sub>	PC/ACN (70:30)

**Table 5.9:** Deposition conditions with associated electrochemical solvents and electrolytes for the monolayer formation of dipyrBEDT-TTF. † PC is propylene carbonate.

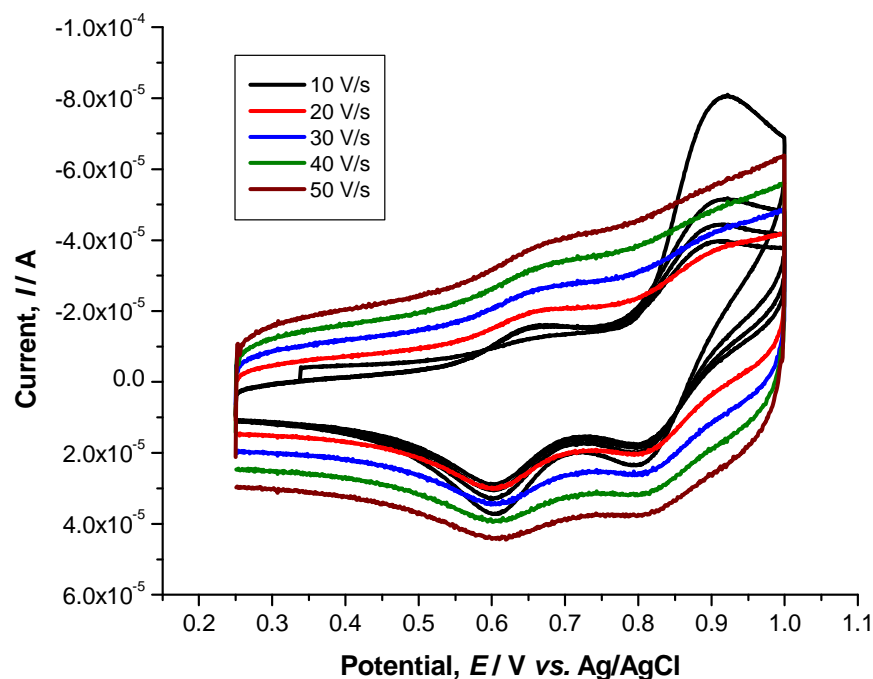


**Figure 5.22:** Cyclic voltammetry of a monolayer of dipyrBEDT-TTF on a Au macro electrode (real surface area =  $0.1041 \text{ cm}^2$ ) following immersion in a  $500 \mu\text{M}$  solution of the compound in  $\text{CH}_2\text{Cl}_2$ , vs. Ag/AgCl, using  $0.1 \text{ M TBAClO}_4$  in acetonitrile.

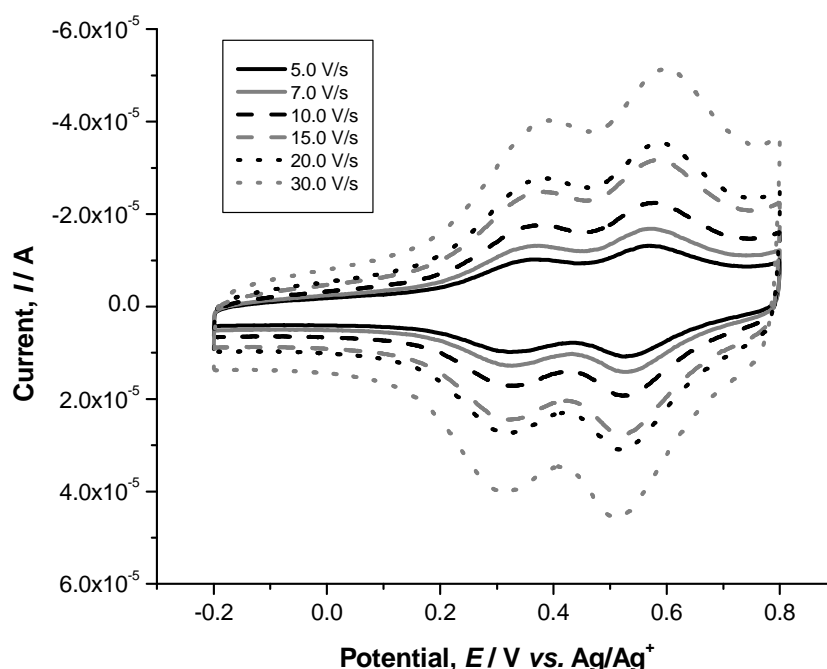
The Faradaic response from the monolayer decreases with each scan rate applied thereafter indicating a decrease in the surface coverage through loss of the compound into the electrolyte solution. This suggests that dipyrBEDT-TTF exhibits a weak affinity for binding to a Au substrate. It must be noted also that the Au surface can be oxidised in the presence of chlorine at potentials close to the oxidation potential of the second redox wave of dipyrBEDT-TTF. Considering a Ag/AgCl reference electrode (3M KCl) was used, the monolayer may have been knocked off the surface as a result of complexation between the Au atoms on the surface and  $\text{Cl}^-$  ions in the solution.<sup>38</sup>

The electrochemical results obtained using both Pt and Au substrates show that dipyrBEDT-TTF exhibits a greater affinity for the Pt surface. Figure 5.23 reveals the electrochemical response observed for a monolayer of the compound on a Pt macro electrode. The electrode, following manual polishing with alumina slurry and

electrochemical cleaning in H<sub>2</sub>SO<sub>4</sub>, was immersed overnight in a 500 μM solution of the compound using DMF/H<sub>2</sub>O (9:1) as the deposition solvent.

An electrochemical characteristic of a surface confined process is a linear relationship between the peak current and the scan rate. Figure 5.23 (bottom graph) reveals this relationship for the monolayer of dipyrBEDT-TTF on Pt under aerobic conditions where the peak current is proportional to the scan rate.

The absence of lateral interactions between adsorbates within a monolayer is indicated by a FWHM of 90.6/n mV and a  $\Delta E_p$  of 0 mV for a one-electron transfer.<sup>51</sup> The  $\Delta E_p$  values observed for the monolayer of dipyrBEDT-TTF (Figure 5.23) are greater than zero with the anodic and cathodic current maxima separated by a minimum of 40 mV ( $v = 7$  V/s) and a maximum of 90 mV ( $v = 30$  V/s). The FWHM calculated for the redox waves in the CV ranges from 120 – 160 mV. As the scan rate increases,  $\Delta E_p$  also increases. A possible reason for this may be that slow charge transfer kinetics is associated with the observed response.<sup>52</sup>



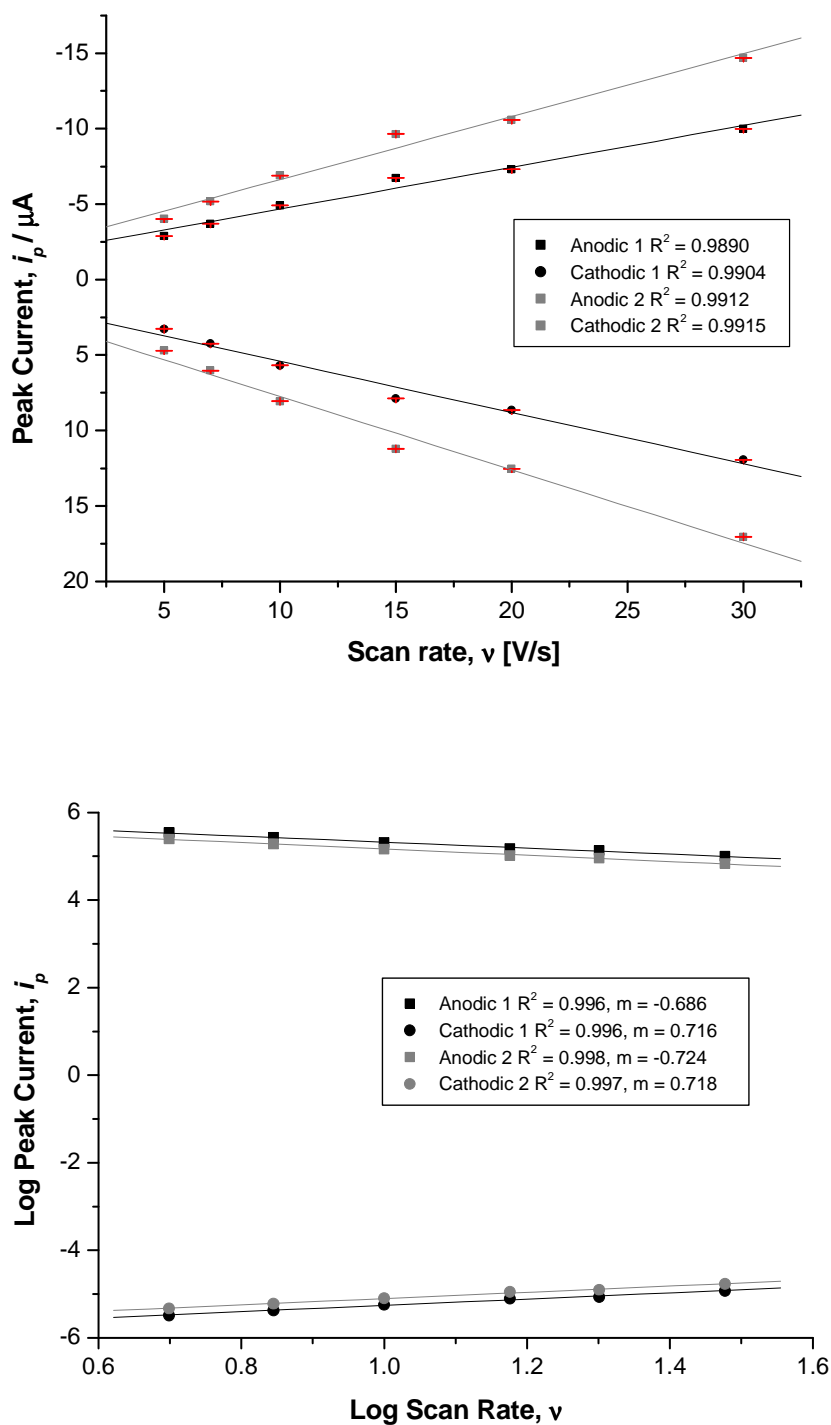


**Figure 5.23:** Cyclic voltammetry of a monolayer of dipyrBEDT-TTF (top) on a Pt electrode (real surface area =  $0.1392 \text{ cm}^2$ ) following immersion in a  $500 \mu\text{M}$  solution of the compound in DMF/ $\text{H}_2\text{O}$  (9:1), vs.  $\text{Ag}/\text{Ag}^+$ , using  $0.1 \text{ M TBABF}_4$  in acetonitrile. Middle graph: illustration of the relationship between the peak current,  $i_p$ , versus the scan rate,  $v$  with  $\log i_p$  vs.  $\log v$  illustrated in the bottom graph.

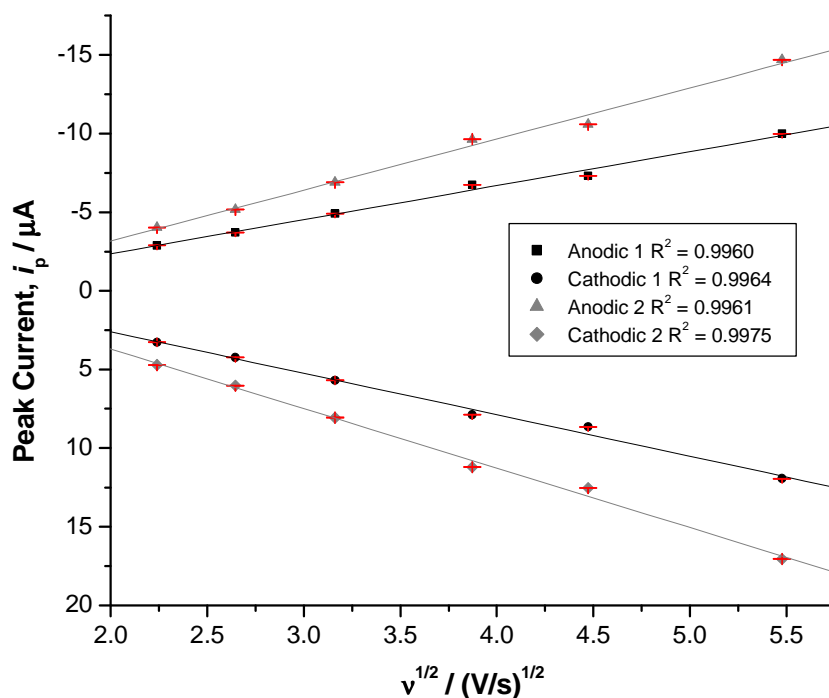


**Figure 5.24:** Graph to illustrate the relationship between the peak current,  $i_p$ , and the square root of the scan rate,  $v^{1/2}$ , for a monolayer of dipyrBEDT-TTF on a Pt electrode (real surface area =  $0.1392 \text{ cm}^2$ ) following immersion in a  $500 \mu\text{M}$  solution of the compound in DMF/ $\text{H}_2\text{O}$  (9:1), vs. Ag/Ag<sup>+</sup>, in  $0.1 \text{ M TBABF}_4$  in acetonitrile.

The influence of diffusion on the electrochemical response from a surface confined species is usually considered to be negligible and therefore it would be assumed that diffusion of the electroactive species to and from the surface of the electrode is excluded as a possible reason for the increased proportionality between the scan rate and  $\Delta E_p$ . However, the linearity of the Randles-Sevcik plot from (equation 2.14, Chapter 2), Figure 5.24, produced from the electrochemical response of the dipyrBEDT-TTF monolayer suggests that diffusion of the species from the surface of the electrode must be considered. The plot of  $i_p$  vs.  $v$  does not equal unity and the presence of the slight curve may indicate that the process may be diffusion controlled to a certain extent. This may explain why an almost immediate decay in the Faradaic current is observed with the monolayer.

However, it is important to note that partial loss of the species from the surface of the electrode, indicated by the decay in the Faradaic current, after the first cyclic

voltammogram will result in attenuation of the Faradaic current observed at the next, higher scan rate. This may lead to a perturbation in the plot of  $i_p$  vs.  $v$ . The electrochemical response therefore may appear to be diffusion controlled when in fact it may be adsorption controlled. This observed decay in the Faradaic current is shown in Figure 5.25.

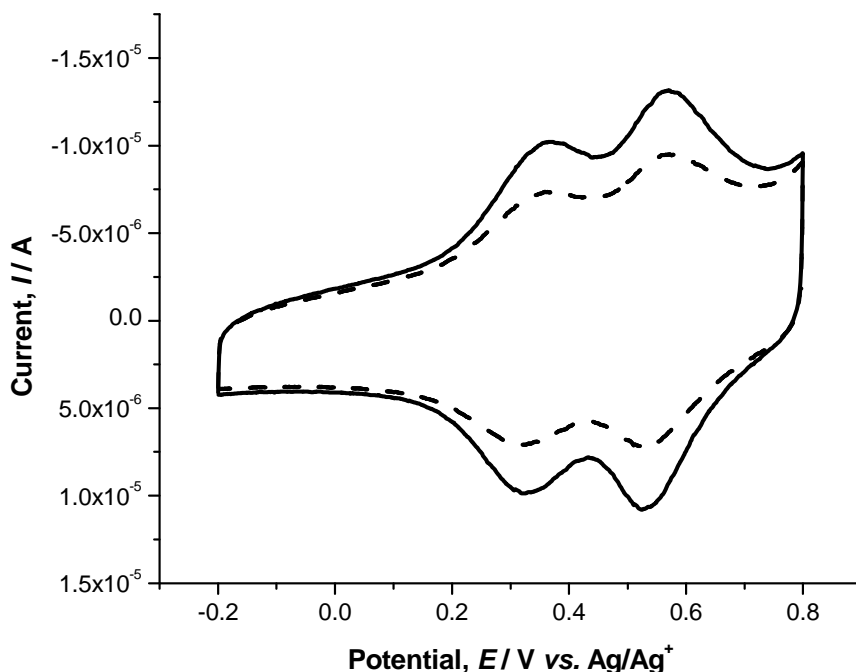


**Figure 5.25:** Demonstration of the lack of stability of the dipyrBEDT-TTF monolayer formed as per conditions outlined in Figure 5.23. The electrochemical response was obtained in an aerobic atmosphere. Solid line: initial scan at 5 V/s. Dashed line: scan at 5 V/s following cycling from 5 to 50 V/s.

In order to obtain some understanding of the packing density of dipyrBEDT-TTF on the Pt surface, the surface coverages of the monolayer under aerobic and anaerobic conditions have been calculated, Table 5.10. The surface coverage was calculated as per Equations 2.19 and 2.23 of Chapter 2. For a dense monolayer, surface coverages in the range of  $10^{-10}$  mol  $\text{cm}^{-2}$  are expected.<sup>51</sup> The value calculated for the dipyrBEDT-TTF monolayer in the presence of oxygen is two orders of magnitude smaller than the optimum value which suggests that a dense monolayer is not formed for this compound on Pt. Comparing the surface coverage calculated for the compound, using

the initial and final scans, it is evident that the density of the monolayer on the surface decreases by approximately 40 % after the potential is applied over the range of scan rates, Figure 5.25.

Scan Rate (V/s)	$\Delta E_p$ (mV) 1 <sup>st</sup> Redox Process	$\Delta E_p$ (mV) 2 <sup>nd</sup> Redox Process	Surface Coverage, $\Gamma$ (mol cm <sup>-2</sup> )
<i>Aerobic Conditions</i>			
5 (Initial Scan)	40	45	$4.86 \pm 0.002 \times 10^{-12}$
5 (Final Scan)	35	45	$2.88 \pm 0.002 \times 10^{-12}$
<i>Anaerobic Conditions</i>			
10 (Initial Scan)	60	80	$1.01 \pm 0.001 \times 10^{-11}$
10 (Final Scan)	60	80	$9.66 \pm 0.01 \times 10^{-12}$

**Table 5.10:**  $\Delta E_p$  and surface coverage of the dipyrBEDT-TTF monolayer on a Pt electrode under aerobic and anaerobic conditions in acetonitrile (0.1 M TBAClO<sub>4</sub>). The final scan was recorded after cycling with scan rates up to 50 V/s (approximately 5 minutes).

The area of the molecule is approximately  $190 \text{ \AA}^2$ <sup>53</sup> and the projected surface area (calculated using equation 3.4 in Chapter 3) of the compound within monolayer is  $3410 \text{ \AA}^2$ . This value is a lot greater than the approximate area of the molecule. A FWHM not equal to  $90.6/n$  mV and a larger than predicted projected area of occupation per molecule suggests that there may be lateral interactions between adsorbates on the surface. However, the surface coverage of the monolayer is in the range of  $10^{-12} \text{ mol cm}^{-2}$  suggesting that a sparse layer is created on the surface of the molecule. The larger value of the FWHM may be associated with non uniform electron transfer rates within the monolayer. As the orientation of the molecule on the surface is yet unknown this possibility of a random disorientated monolayer must be considered.

In order to adequately characterise monolayers on a surface using different techniques, stable systems where the compound remains tightly bound to the substrate, offer a significant advantage. The decay in the Faradaic current observed for the monolayer

when the electrochemistry was carried out in air is not ideal in the pursuit of developing molecular components.

A lack of stability was observed for all monolayers of dipyrBEDT-TTF assembled on Pt and Au electrodes in an aerobic atmosphere. Unfortunately, upon applying a potential and oxidising the compound on the surface to the monocation radical, and subsequently to the dication, decay in the Faradaic current was observed. This decay current was observed for all experimental conditions outlined in Table 5.9 when the electrochemistry was carried out in the presence of oxygen. However, akin to the results obtained for the cyclic voltammetry of dipyrBEDT-TTF in the solution-phase diffusion controlled experiments, it was expected that by obtaining an anaerobic atmosphere prior to applying a potential, this Faradaic current decay would not be observed.

A deposition solvent mix of DMF and H<sub>2</sub>O (9:1) was used in the formation of the dipyrBEDT-TTF monolayer shown in Figure 5.23. A monolayer of this compound, formed by immersing a Pt electrode in an alternative solvent (CH<sub>2</sub>Cl<sub>2</sub>) is shown in Figure 5.26. Cyclic voltammetry of this monolayer was recorded under anaerobic conditions: the cell was initially purged with argon and a blanket of the gas was maintained throughout the experiment. As was observed for the monolayer in the presence of oxygen, the  $\Delta E_p$  values observed are greater than zero and the anodic and cathodic current maxima are separated by a minimum of 60 mV ( $v = 10$  V/s) and 80 mV ( $v = 50$  V/s).

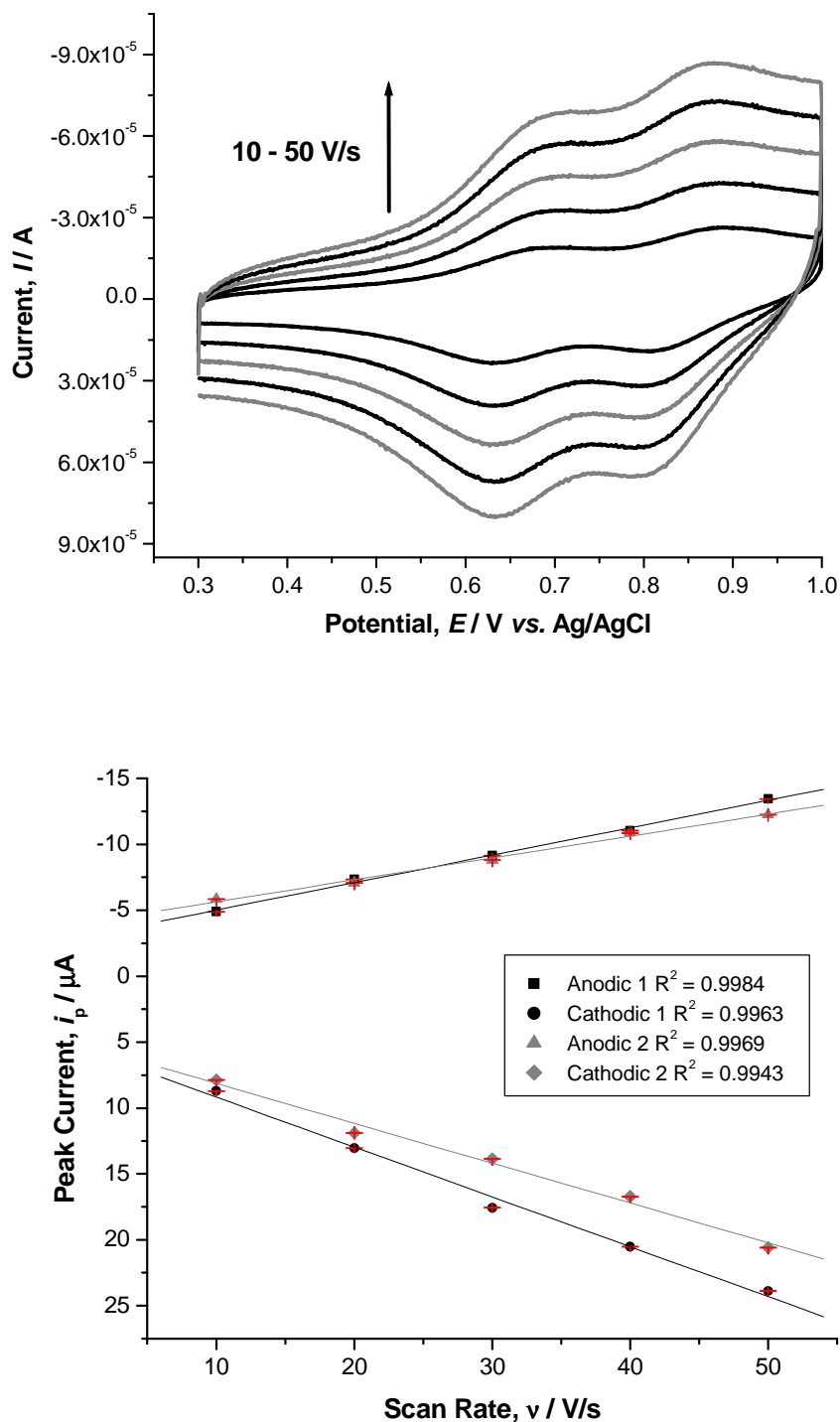


**Figure 5.26:** Cyclic voltammetry of a monolayer of dipyrBEDT-TTF (top) on a Pt electrode (real surface area =  $0.116 \text{ cm}^2$ ) following immersion in a  $500 \mu\text{M}$  solution of the compound in  $\text{CH}_2\text{Cl}_2$ , vs. Ag/AgCl, using  $0.1 \text{ M TBAClO}_4$  in acetonitrile. CVs were recorded under argon. Bottom graph: illustration of the linear relationship between the peak current,  $i_p$ , versus the scan rate,  $v$ .

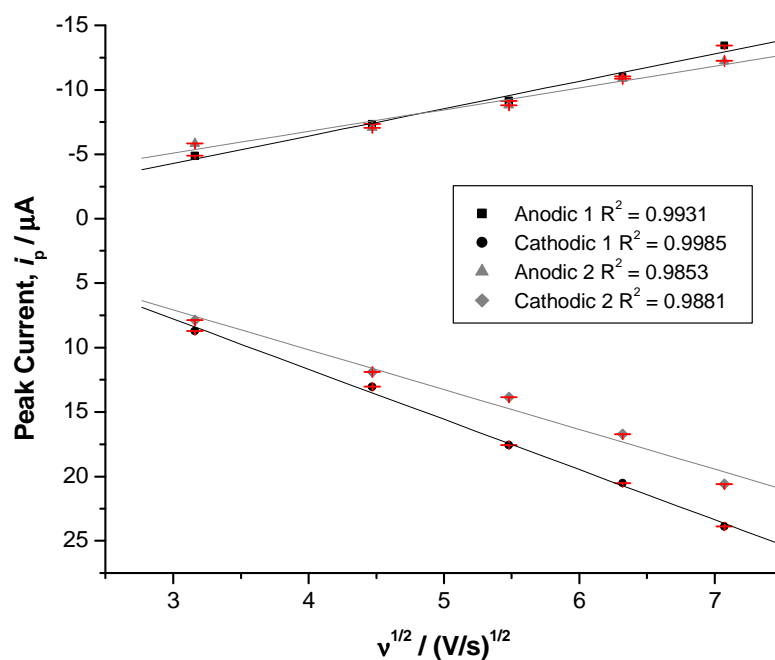


**Figure 5.27:** Graph to illustrate the relationship between the peak current,  $i_p$ , and the square root of the scan rate,  $v^{1/2}$ , for a monolayer of dipyrBEDT-TTF on a Pt electrode (real surface area =  $0.116 \text{ cm}^2$ ) following immersion in a  $500 \mu\text{M}$  solution of the compound in  $\text{CH}_2\text{Cl}_2$ , vs. Ag/AgCl, using  $0.1 \text{ M TBAClO}_4$  in acetonitrile.

The FWHM calculated for the redox waves in the CV ranges from 110 – 140 mV. Figure 5.26 (bottom) reveals the relationship between the peak current and the scan rate for the monolayer of dipyrBEDT-TTF in the absence of oxygen; a linear relationship is observed. Increasing the scan rate from 10 – 50 V/s results in minimal changes in the peak potential ( $E_p$ ). This absence of proportionality between the scan rate and  $\Delta E_p$  was not observed for the monolayer under aerobic conditions where  $\Delta E_p$  increased with increasing scan rate. A possible reason for this response may be that the electron transfer kinetics for the monolayer in an aerobic environment is more sluggish than that of the monolayer in the absence of oxygen.<sup>52</sup>

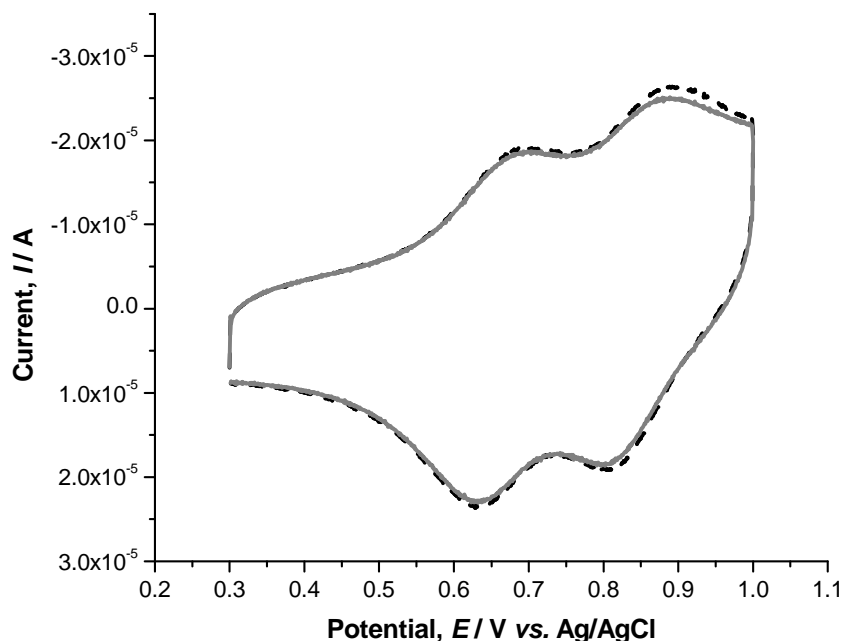


**Figure 5.28:** Cyclic voltammogram of the dipyrBEDT-TTF monolayer formed as per conditions outlined in Figure 5.26. The electrochemical response was obtained in the absence of oxygen. Dashed black line: initial scan at 10 V/s, solid grey line: scan at 10 V/s following scanning from 10 to 50 V/s.

Under solution-phase diffusion controlled conditions the dipyrBEDT-TTF dication is unstable in the presence of oxygen. The lack of stability of dipyrBEDT-TTF monolayer, under aerobic conditions, is also observed. A possible reason for this phenomenon includes a proceeding chemical reaction between molecular oxygen and the electrochemically generated dication dipyrBEDT-TTF<sup>2+</sup>; *vide supra*.<sup>47</sup> Considering the significant improvement in the stability of the monolayer in an oxygen free environment (Figure 5.28) it is possible that similar chemical reactions occur for the oxidised monolayer which hinder the compounds ability to remain on the surface.

The surface coverages for the monolayer, shown in Figure 5.26, have been calculated for the initial and final cycles, each at a scan rate of 10 V/s, Table 5.10. A value of  $1.01 \pm 0.001 \times 10^{-11} \text{ mol cm}^{-2}$  represents the surface coverage for the initial scan at 10 V/s with a projected area per molecule of  $1640 \text{ \AA}^2$ . The monolayer was then cycled at

scan rates up to 50 V/s before final scanning at 10 V/s. The surface coverage for this final scan is  $9.66 \pm 0.01 \times 10^{-12}$  mol cm<sup>-2</sup>. Considering that a loss of up to 40% of the monolayer was observed in the presence of oxygen, it may be concluded that an oxygen free environment significantly improves stability.

The calculated surface coverage for the monolayer in the oxygen free environment is significantly greater than that of the monolayer in the presence of oxygen, Table 5.10. Two different solvent systems were used in the formation of each monolayer. The latter was formed using DMF/H<sub>2</sub>O (90:10) with the former immersed in a CH<sub>2</sub>Cl<sub>2</sub> solution of the compound. The dipyrBEDT-TTF compound is insoluble in H<sub>2</sub>O which is expected as it is a neutral organic compound and H<sub>2</sub>O is a highly polar solvent. The presence of H<sub>2</sub>O in the immersion solution resulted in limited solubility whereas the molecule is more soluble in CH<sub>2</sub>Cl<sub>2</sub>. The increased solubility in the latter may explain the greater surface coverage for the monolayer shown in Figure 5.26.

### 5.3 Conclusions

This chapter has focused on the electrochemical characterisation and monolayer formation of a TTF derivative, dipyrBEDT-TTF as it is potentially useful as a conducting molecular component for electronic devices. Two anodic redox processes have been observed in the solution-phase diffusion controlled electrochemistry of dipyrBEDT-TTF, both of which are reversible and characteristic of TTF type compounds. The first (least positive) of these oxidative processes represents the oxidation of the neutral compound to the monocation radical followed by the removal of a second electron forming a dication, Figure 5.9. Two irreversible cathodic processes are also observed in the CV at negative potentials both of which are proposed to be centred on the pyridine rings; reduction potentials for the TTF core generally reported to occur outside the experimental potential ranges<sup>34, 35, 54</sup> used which may be due to its electron rich character.

The diffusion controlled electrochemical response of dipyrBEDT-TTF was examined in the presence of different electrolyte solvents which include CH<sub>2</sub>Cl<sub>2</sub>, DMF, THF and acetone. The effect of each solvent on the potentials of the first and second redox processes, and the stability of the monocation intermediate ( $\Delta E$ ), has been investigated. No correlation was observed in the examination of the effect of polarity, dielectric constant and Gutmann acceptor number on the first redox potential and  $\Delta E$ . However, it was observed that as the Gutmann donor number of the solvent increased, the stability of the redox intermediate decreased, leading to an inversely proportional relationship between the donor number and  $\Delta E$ , Table 5.5 and Figure 5.15. This is because the increased donor strength of solvents such as acetone and DMF make it thermodynamically easier to remove a second electron and oxidise the monocation radical to the dication state.

By examining the redox processes in dichloromethane, both in aerobic and anaerobic environments, it was observed that the stability of the dication is highly sensitive to the presence of oxygen in the electrochemical cell. The stability of the monocation radical was found to be independent of oxygen and as such it was proposed that the observed degradation of the compound (Figure 5.16 (top)) originates from an

interaction of the dication (most likely at the sulphur heteroatom of the TTF core) with molecular oxygen.

The stability of the monocation radical was confirmed through spectroelectrochemical experiments. Several bands are observed in the absorbance spectra of dipyrBEDT-TTF. The lower energy bands at 31650 and 28900  $\text{cm}^{-1}$  (316 and 346 nm respectively) are a common feature in the spectra of this type of compound. Two absorbance bands, of similar wavelength, are also observed in the absorbance spectra of the reference compound BEDT-TTF<sup>48</sup> (324 and 349 nm) and are reported to represent a transition from the HOMO ( $\pi$ ) to the LUMO ( $\sigma^*$ ) (349 nm) with the higher energy wave corresponding to a HOMO to LUMO+1  $\pi \rightarrow \pi^*$  transition.

Electrochemical oxidation of dipyrBEDT-TTF to the monocation radical is accompanied by a decrease in the absorbance bands at 43860, 39680, 31650 and 28900  $\text{cm}^{-1}$  (Figure 5.19) with the appearance and concomitant increase in new absorbance bands at 23585, 21880, 20875, 17825 and 10820  $\text{cm}^{-1}$  (424, 457, 479, 561 and 924 nm), Figure 5.20. The nature of the absorbance band at 924 nm is unclear and in order to assign this band as that of an intervalence transition further spectroelectrochemical measurements in an anaerobic environment are required. Reduction of the monocation to the neutral dipyrBEDT-TTF leads to the observation that this first oxidation is fully reversible (Figure 5.21) and the monocation is stable as indicated by the electrochemical results.

The electrochemical response and stability of dipyrBEDT-TTF on the surface of metal electrodes was examined by forming monolayers of the compound on Pt and Au substrates. The use of a Au electrode results in a highly unstable monolayer. When a potential is applied and the compound is oxidised to the dication the Faradaic current quickly decays indicating that the compound is being removed from the surface. A significantly improved electrochemical response is obtained using a Pt electrode as the substrate for monolayer formation. The resulting monolayer exhibits a linear relationship between the peak current,  $i_p$  and the scan rate,  $v$  characteristic of surface confined process. The monolayer of dipyrBEDT-TTF on Pt reveals a FWHM of greater than 90.6 mV and a non-zero value is calculated for the separation between the anodic and cathodic current maxima,  $\Delta E_p$ . In the presence of oxygen the stability of

the monolayer is poor with decay in the Faradaic current observed upon successive cycling at different scan rates. Exploring this phenomenon in an anaerobic environment resulted in a significant increase in the stability of the monolayer. The molecule exhibits a surface coverage of  $1.01 \pm 0.001 \times 10^{-11} \text{ mol cm}^{-2}$  on a Pt surface indicating that an incomplete monolayer has been formed.

Upon initial evaluation of dipyrBEDT-TTF, it was proposed that this molecule would be potentially useful as a molecular diode for electronic devices. There are two main reasons for this, the first of which is the existence of two readily accessible redox states within the molecule. Secondly, there are several sites for the binding to an electrode surface – a necessity for measuring molecular conductivity between an adsorbate-substrate interface. The molecule may anchor to the surface in an upright position through the pyridine rings, on its side through sulphur (although steric hindrance would likely impede this) or lying flat through interaction between the eight sulphur atoms and the electrode surface.

The characterisation of the molecule's orientation on the surface, the mechanism of electron transfer to and from the electrode and the molecular conductivity can be determined using *in situ* electrochemical STM. Unfortunately, these measurements could not be carried out in the conditions where the monolayer demonstrates stability on the surface. Time limitations have prevented further efforts with this experiment.

## 5.4 Bibliography

---

- 1 Feynman, R.P., *Eng. Sci.*, **1960**, 23, 22.
- 2 (a) Wudl, F., Smith, G.M., Hufnagel, E. J., *Chem. Commun.*, **1970**, 1453, (b)  
Wudl, F., Wobschal, D., Hufnagel, E.J., *J. Am. Chem. Soc.*, **1972**, 94, 670.
- 3 Aviram, A., Ratner, M.A., *Chem. Phys. Lett.*, **1974**, 29, 277.
- 4 Hunig, S., Schlaf, H., Kiesslick, G., Schentzow, D., *Tetrahedron Letters*, **1969**,  
2271.
- 5 The reversible oxidation of the TTF core was observed electrochemically  
using cyclic voltammetry in acetonitrile, reference 4.
- 6 Bendikov, M., Wudl, F., Perepichka, D.F., *Chem. Rev.*, **2004**, 104, 4891.
- 7 Cooper, W.F., Kenny, N.C., Edmonds, J.W., Nagel, A., Wudl, F., Coppens, P.,  
*Chem. Commun.*, **1971**, 889.
- 8 Bryce, M.R., *Adv. Mater.*, **1999**, 11, 11.
- 9 Ferraris, J., Cowan, D.O., Walatka, V., Perlstein, J.H., *J. Am. Chem. Soc.*,  
**1973**, 95, 948.
- 10 Mizuseki, H., Igarashi, N., Majumder, C., Belosludov, R.V., Farajian, A.A.,  
Kawazoe, Y., *Thin Solid Films*, **2003**, 438, 235.
- 11 Joachim, C., Gimzewski, J.K., Aviram, A., *Nature*, **2000**, 408, 541.
- 12 Ho, G., Heath, J.R., Kondratenko, M., Perepichka, D.F., Arseneault, K.,  
Pezolet, M., Bryce, M.R., *Chem. Eur. J.*, **2005**, 11, 2914.
- 13 Metzger, R., *Mater. Sci. and Eng.*, **1995**, C3, 277.

- 14 (a) Metzger, R.M., Panetta, C.A., *Molecular Electronic Devices*, Marcel Dekker, New York, USA, **1987**, (b) Ashwell, G.J., Sage, I., Trundle, C., *Molecular Electronics*, Wiley, New York, USA, **1992**, (c) Metzger, R.M., *Annals New York Acad. Sci.*, **2003**, *1006*, 252, (d) Panetta, C.A., Baghdadchi, J., Metzger, R.M., *Mol. Cryst. Liq. Cryst.*, **1984**, *107*, 103, (e) de Miguel, P., Bryce, M.R., Goldenburg, L.M., Beeby, A., Khodorkovsky, V., Shapiro, L., Niemz, A., Cuello, A.O., Rotello, V., *J. Mater. Chem.*, **1998**, *8*, 71, (f) Scheib, S., Cava, M.P., Baldwin, J.W., Metzger, R.M., *J. Org. Chem.*, **1998**, *63*, 1198, (g) Tsiperman, E., Becker, J.Y., Khodorkovsky, V., *Tetrahedron Letts.*, **2007**, *48*, 4161.
- 15 (a) Brooks, A.C., Day, P., Dias, S.I.G., Rabaca, S., Santos, I.C., Henriques, R.T., Wallis, J.D., Almeida, M., *Eur. J. Inorg. Chem.*, **2009**, 3084, (b) Brooks, A.C., Day, P., Wallis, J.D., *Acta. Cryst.*, **2008**, *C64*, 245, (c) Wang, Q., Day, P., Griffiths, J.P., Nie, H., Wallis, J.D., *New J. Chem.*, **2006**, *30*, 1790, (d) Wallis, J.D., Griffiths, J.P., *J. Mater. Chem.*, **2005**, *15*, 347, (e) Griffiths, J.P., Nie, H., Brown, R.J., Day, P., Wallis, J.D., *Org. Biomol. Chem.*, **2005**, *3*, 2155, (f) Griffiths, J.P., Brown, R.J., Day, P., Matthews, C.J., Vital, B., Wallis, J.D., *Tetrahedron Letters*, **2003**, *44*, 3127, (g) Xu, W., Zhang, D., Li, H., Zhu, D., *J. Mater. Chem.*, **1999**, *9*, 1245.
- 16 Rovira, C., *Chem. Rev.*, **2004**, *104*, 5289.
- 17 Williams, J.M., Schultz, A.J., Geiser, U., Carlson, K.D., Kini, A.M., Wang, H.M., Kwok, W.K., Whangbo, M.H., Shirber, J.E., *Science*, **1991**, *252*, 1501.
- 18 Hervé, K., Liu, S., Cador, O., Golhen, S., Le Gal, Y., Bousseksou, A., Stoeckli-Evans, H., Decurtins, S., Ouahab, L., *Eur. J. Inorg. Chem.*, **2006**, 3498.
- 19 Jia, C., Zhang, D., Xu, Y., Xu, W., Hu, H., Zhu, D., *Synthetic Metals*, **2003**, *132*, 249.

- 20 (a) Haiss, W., van Zalinge, H., Higgins, S.J., Bethell, D., Höbenreich, H., Schiffrin, D.J., Nichols, R.J., *J. Am. Chem. Soc.*, **2003**, *125*, 15294, (b) Haiss, W., van Zalinge, H., Höbenreich, H., Bethell, D., Schiffrin, D.J., Higgins, S.J., Nichols, R.J., *Langmuir*, **2004**, *20*, 7694, (c) Haiss, W., Albrecht, T., van Zalinge, H., Higgins, S.J., Bethell, D., Höbenreich, H., Schiffrin, D.J., Nichols, R.J., Kuznetsov, A.M., Zhang, J., Chi, Q., Ulstrup, J., *J. Phys. Chem. B*, **2007**, *111*, 6703.
- 21 (a) Li, Z., Han, B., Meszaros, G., Pobelov, I., Wandlowski, T., Blaszczyk, A., Mayor, M., *Faraday Discuss.*, **2006**, *131*, 121, (b) Gittins, D.I., Bethell, D., Schiffrin, D.J., Nichols, R.J., *Nature*, **2000**, *408*, 67, (c) Xu, B.Q., Xiao, X.Y., Yang, X.M., Zang, L., Tao, N.J., *J. Am. Chem. Soc.*, **2005**, *127*, 2386, (d) Chen, F., He, J., Nuckolls, C., Roberts, T., Klare, J.E., Lindsay, S., *Nano Lett.*, **2005**, *5*, 503, (e) Albrecht, T., Guckian, A., Ulstrup, J., Vos, J.G., *IEEE Trans*, **2005**, *4*, 430, (f) Albrecht, T., Guckian, A., Ulstrup, J., Vos, J.G., *Nano Letters*, **2005**, *5*, 1451, (g) Albrecht, T., Moth-Poulsen, K., Christensen, J.B., Guckian, A., Bjornholm, T., Vos, J.G., Ulstrup, J., *Faraday Discussions*, **2006**, *131*, 265, (h) Albrecht, T., Guckian, A., Kuznetsov, A.M., Vos, J.G., Ulstrup, J., *J. Am. Chem. Soc.*, **2006**, *128*, 17132.
- 22 (a) Gittins, D.I., Bethell, D., Nichols, R.J., Schiffrin, D.J., *J. Mater. Chem.*, **2000**, *10*, 79, (b) Monk, P.M.S., *The Viologens*, Wiley, Chichester, **1998**
- 23 Leary, E., Higgins, S.J., van Zalinge, H., Haiss, W., Nichols, R.J., Nygaard, S., Jeppesen, J.O., Ulstrup, J., *J. Am. Chem. Soc.*, **2008**, *130*, 12204.
- 24 Fletcher, D.A., McMeeking, R.F., Parkin, D.J., *J. Chem. Inf. Comput. Sci.*, **1996**, *36*, 746.
- 25 Bockman, T.M., Kochi, J.K., *J. Org. Chem.*, **1990**, *55*, 4127.
- 26 Gomar-Nadal, E., Ramachandran, G.K., Chen, F., Burgin, T., Rovira, C., Amabilino, D.B., Lindsay, S.M., *J. Phys. Chem. B*, **2004**, *108*, 7213.

- 27 Ramachandran, G.K., Tomfohr, J.K., Li, J., Sankey, O.F., Zarate, X., Primak, A., Terazano, Y., Moore, T.A., Moore, A.L., Gust, D., Nagahara, L.A., Lindsay, S.M., *J. Phys. Chem. B*, **2003**, *107*, 6162.
- 28 Wold, D.J., Haag, R., Rampi, M.A., Frisbie, C.D., *J. Phys. Chem. B*, **2002**, *106*, 2813.
- 29 (a) Henning, T.P., White, H.S., Bard, A.J., *J. Am. Chem. Soc.*, **1981**, *103*, 3937, (b) Schott, J.H., Yip, C.M., Ward, M.D., *Langmuir*, **1995**, *11*, 177.
- 30 Yip, C.M., Ward, M.D., *Langmuir*, **1994**, *10*, 549.
- 31 Fujihara, H., Nakai, H., Yoshihara, M., Maeshima, T., *Chem. Comm.*, **1999**, 737.
- 32 Moore, A.J., Goldenburg, L.M., Bryce, M.R., Petty, M.C., Moloney, J., Howard, J.A.K., Joyce, M.J., Port, S.N., *J. Org. Chem.*, **2000**, *65*, 8269.
- 33 Hurtley, W.R.H., Smiles, S., *J. Chem. Soc.*, **1926**, 2263.
- 34 Qiu, H, Wang, C., Xu, J., Lai, G., Shen, Y., *Monatsh Chem*, **2008**, *139*, 1357.
- 35 Gonzilez, M., Illescas, B., Martín, N., Segura, J.L., Seoane, C., Hanack, M., *Tetrahedron*, **1998**, *54*, 2853.
- 36 Cisak, A., Elving, P.J., *Electrochimica Acta*, **1965**, *10*, 935.
- 37 Bard, A.J., Faulkner, L.R., *Electrochemical Methods, Fundamentals and Applications*, 2<sup>nd</sup> Ed., John Wiley & Sons, Inc., USA, **2001**.
- 38 Sawyer, D.T., Sobkowiak, A., Roberts Jr., J. L., *Electrochemistry for Chemists*, 2<sup>nd</sup> Ed., John Wiley & Sons, USA, **1995**.

- 39 Matsuda, H., Ayabe, Y., *Z. Electrochem.*, **1955**, 59, 494.
- 40 Barrière, F., Kirss, R.U., Geiger, W.E., *Organometallics*, **2005**, 24, 48.
- 41 Gutmann, V., *The Donor-Acceptor Approach to Molecular Interactions*, Plenum, New York, USA, **1978**.
- 42 Hill, J.W., Petrucci, R.H., *General Chemistry – An Integrated Approach*, 3<sup>rd</sup> Ed., Prentice – Hall, Inc., New Jersey, USA, **2002**.
- 43 Skoog, D.A., Holler, F.J., Nieman, T.A., *Principles of Instrumental Analysis*, 5<sup>th</sup> Ed., Harcourt Brace & Company, Florida, USA, **1998**.
- 44 Lide, D.R., *Handbook of Organic Solvents*, CRC Press, Florida, USA, **1995**.
- 45 Gutmann, V., *Lecture Notes on Solution Chemistry*, World Scientific, **1995**.
- 46 (a) Browne, W.R., de Jong, J.J.D., Kudernac, T., Walko, M., Lucas, L.N., Uchida, K., van Esch, J.H., Feringa, B.L., *Chem. Eur. J.*, **2005**, 11, 6414, (b) D'Alessandro, D.M., Keene, F.R., *J. Chem. Soc. Dalton. Trans.*, **2004**, 3950, (c) Yeomans, B.D., Kelso, L.S., Tregloan, P.A., Keene, F.R., *Eur. J. Inorg. Chem.*, **2001**, 239.
- 47 (a) Bailey, W.J., Cummins, E.W., *J. Am. Chem. Soc.*, **1954**, 76, 1932, (b) Schöneich, C., Aced, A., Asmus, K.D., *J. Am. Chem. Soc.*, **1993**, 115, 11376, (c) Miller, B.L., Williams, T.D., Schöneich, C., *J. Am. Chem. Soc.*, **1996**, 118, 11014, (d) Arbizzani, C., Mastragostino, M., Soavi, F., *Electrochimica Acta*, **2000**, 45, 2273.
- 48 Andreu, R., Garín, J., Orduna, J., *Tetrahedron*, **2001**, 57, 7883.
- 49 Browne, W.R., Hage, R., Vos, J.G., *Coord. Chem. Rev.*, **2006**, 250, 1653.

- 50 Creutz, C., *Progress of Inorganic Chemistry*, ed. S. J. Lippard, Wiley, New York, USA, **1983**.
- 51 Forster, R.J., Keyes, T.E., Vos, J.G., *Interfacial Supramolecular Assemblies*, John Wiley & Sons Ltd., Chichester, England, **2003**.
- 52 Forster, R.J., Faulkner, L.R., *J. Am. Chem. Soc.*, **1994**, *116*, 5444.
- 53 Personal communication, James Walsh, Professor Tia E. Keyes research group, Dublin City University. The approximate surface area was calculated using Hyperchem software, version 7.1.
- 54 Dolder, S., Liu, S.X., Neels, A., Labat, G., Decurtins, S., *J. Low Temp. Physics*, **2006**, *142*, 457.